Impact of Supercritical CO_2 on Shale Reservoirs and Its Implication for CO_2 Sequestration

Hazra, Bodhisatwa; Vishal, Vikram; Sethi, Chinmay; Chandra, Debanjan

DOI
10.1021/acs.energyfuels.2c01894

Publication date
2022

Document Version
Final published version

Published in
Energy and Fuels

energy&fuels

pubs.acs.org/EF

Review

Impact of Supercritical CO_2 on Shale Reservoirs and Its Implication for CO_2 Sequestration

Bodhisatwa Hazra, Vikram Vishal,* Chinmay Sethi, and Debanjan Chandra

Cite This: *Energy Fuels* 2022, 36, 9882−9903

Read Online

ACCESS | Metrics & More | Article Recommendations

ABSTRACT: Hydraulic fracturing has transformed the international energy landscape by becoming the go-to method for the exploitation of natural gas from unconventional shale reservoirs. However, in the recent years, the search for an alternative method of shale-gas exploration has intensified, because of various problems (e.g., contamination of ground and surface water, overexploitation of precious water resources, air pollution, etc.) associated with the usage of water-based fracturing techniques. The use of CO_2 for shale gas exploitation has emerged as a better alternative to aqueous-based gas exploration techniques. CO_2 when injected into deep shale reservoirs, transitions into supercritical CO_2 (SC-CO_2) when temperature and pressure condition exceeds the critical point, i.e., 31.1 °C and 7.38 MPa. In this paper, we comprehensively review the impact of SC-CO_2 on shale gas reservoirs during the different stages of shale-gas exploration, i.e., (i) drilling, which involves the superiority of SC-CO_2 over water-based drilling fluids, in terms of achieving underbalanced well condition, higher rates of penetration, and resistance to formation damage; (ii) fracturing, which involves factors affecting the tortuosity of fractures created by SC-CO_2 fracturing, breakdown pressure, and proppant-carrying capacity; and (iii) injection, which involves the twin-headed benefit of enhanced recovery due to CO_2/CH_4 competitive adsorption and geological sequestration, CO_2 vs CH_4 excess sorption as a function of pressure, etc. Several research works have indicated discrepancies on how SC-CO_2 impacts different shale properties. Some studies show low-pressure N_2-gas-adsorption-derived surface area and total pore volume to be increasing with SC-CO_2 imbibition, while others show a decreasing trend for the same. Similarly, for some shales, the quartz content, along with the clay mineral contents, decreased as the exposure to SC-CO_2 increased, while in some other studies, with similar long-term exposure to SC-CO_2, the quartz content was observed to increase along with the decrease in clay content and vice versa. Essentially, the increased exposure to SC-CO_2 results in the dissolution of primary porous structures and fractures, and reformation of newer porous structure and conduits in shales. Nonetheless, these changes in the mineralogy weaken the microstructure of the rock bringing significant changes in the mechanical properties of the shales with implications on the wellbore stability and fracturing efficiency. The mechanical properties such as uniaxial compressive strength (UCS), Young's modulus, and tensile strength decrease as the SC-CO_2 saturation period increases. However, some studies have shown factors like bedding angle and phase-state of CO_2 having varying effect on the strength behavior of the shales. Moreover, changes in the structure of shales caused by the creation of fractures and the reduction of their strength can also pose major risks, because of potential leakage of CO_2 through these created pathways. How these processes would interact at field scale would control the sealing capacity, especially at field-scale for addressing long-term seepage of CO_2.

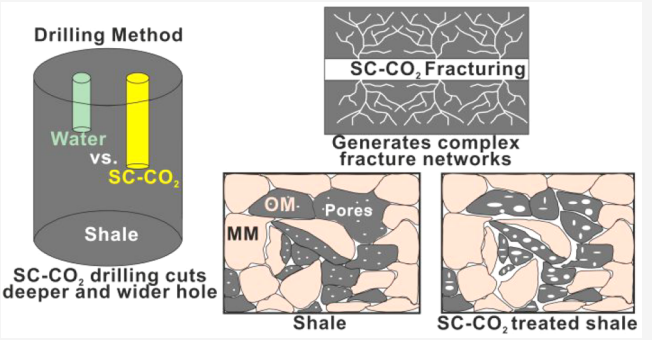

1. INTRODUCTION

To meet the global energy requirements of large and developing populations, the past few decades have seen increased application of fossil fuels globally.[1] While fossil fuels have primarily contributed toward improvement in the quality of life, its combustion has also resulted in a sharp increase in emission of greenhouse gases (GHGs) to the atmosphere. This increased contribution from the fossil fuels toward atmospheric emissions, has been identified as one of the major causes for global warming and climate change in the recent years.[2] Time and again, conventional fossil fuel sources such as coal, petroleum, and others have been highlighted to be the major contributors toward GHG emission. For example, fossil fuel-based power plants, contributes almost $^1/_3$ of the total CO_2 release/year

Received: June 7, 2022
Revised: July 29, 2022
Published: August 23, 2022

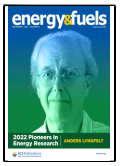

globally.[3] In comparison to the burning of coal and oil, the usage of natural gas has been seen to be a greener energy option as it induces approximately 45% lower CO_2 emissions.[4] Unconventional shale petroleum systems and other tight gas systems, have thus received renewed tremendous research impetus in recent years for its emergence as a vast and cleaner energy option, and also for their gas storage properties.[5−7] However, the rising anthropogenic contributions to atmospheric CO_2 leading to fast environmental changes has been identified globally. In 2015, in one of the most ambitious climate change meetings held at France, with representatives of 190+ countries, the 2015 Paris Climate Agreement (PCA) was signed with the objective to prevent global temperature increase to 2 °C above preindustrial levels, and make strides en route for attaining 1.5 °C temperature stabilization.[8]

It is self-explanatory that, for the progress of civilization, utilization of available energy resources cannot be terminated, and to accommodate this with the PCA objective, negative GHG emissions is to be achieved in the coming decades.[9−12] Luderer et al.[13] estimated that, even after phenomenal efforts by several countries, the fossil fuel contribution to emission until the end of century would remain ∼1000 Gt CO_2. In this context, carbon capture and storage (CCS) in geological reservoirs has been identified as a feasible near-term option to combat the rising GHG emissions.[8,14−20]

Injection of CO_2, for enhanced oil recovery (EOR), is an interesting option and has been in place for the last several decades. Orr and Taber[21] reviewed the applicability of CO_2 injection in conventional oil reservoirs and the principal mechanisms that are operative for EOR. They correctly predicted large-scale worldwide usage of CO_2 injections for EOR in the future. Since the early 1990s, several small and large-scale field-based projects have been executed in multiple nations, which has explored and helped in improving the understandings on storing CO_2 in conventional reservoirs.[18,19] One of the major reasons why deep conventional reservoirs have worked as well-defined targets is the presence of impervious or low-permeability cap-rocks, which arrests the flowage of CO_2 to shallower levels.[22]

The emergence of unconventional reservoirs, especially shale petroleum systems, has not only altered the "geopolitics" around global oil and gas supply need, but has also been recognized as a promising target for CCS.[5,23] As established, shale hydrocarbon systems are a source as well as a reservoir for hydrocarbons, and the hydrocarbons are primarily stored through the basic mechanism of "adsorption", in addition to existing in free and dissolved states.[25] In addition to the enormous hydrocarbon reserve that unconventional shales petroleum systems have, their ability to store hydrocarbons has triggered the interest of many as potential targets for CCS.[25−29] The type, amount, and maturity of organic matter (which generates hydrocarbons and stores them primarily), mineral matter (stores hydrocarbons secondarily), pore structural properties (viz. surface area, pore volume, pore heterogeneity, fractal dimensions, etc.), depth of occurrence and thickness of the deposits, are identified as the critical factors considered from evaluating hydrocarbon producibility and CO_2 storability in shales.[5,28,30−34] Because of their large resources, cleaner energy option, and CCS potential, unconventional shales have been identified as a possible bridge toward our transition to renewable energy resources.[34]

The CO_2, when injected in deep shale or other reservoirs, undergo phase transition to supercritical state beyond its critical point at 31.1 °C and 7.38 MPa, and is known as supercritical CO_2 (SC-CO_2). Figure 1 displays the phase transition diagram

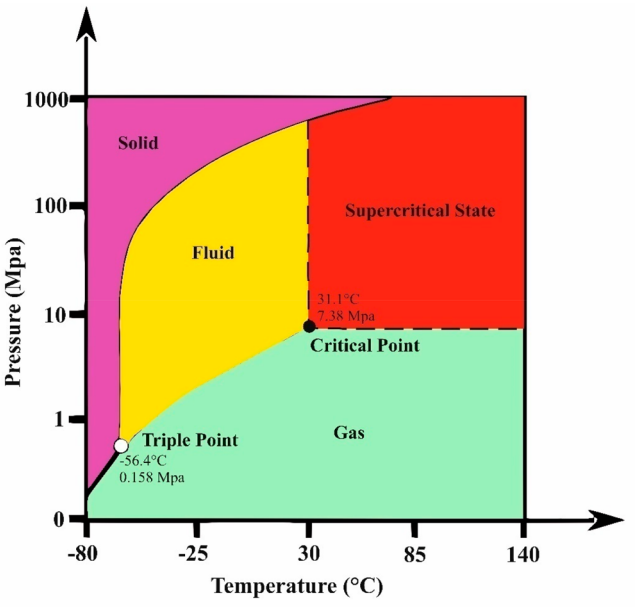

Figure 1. Phase transition diagram of CO_2 [adapted with permission from Yang et al.[36]].

of CO_2.Different researchers have demonstrated the interaction mechanism of SC-CO_2. By virtue of its distinctive properties, the main mechanisms through which SC-CO_2 affects shale reservoir are, through extraction of organic matter, adsorption-induced swelling, and mineral dissolution.[35] These interactions cause the creation of wider and extended fractures, and they enhance hydrocarbon recovery. SC-CO_2 has much higher penetration capacity, in comparison to water-based fracking fluids. Even further, the degree of clay swelling is also lower when shales are exposed to SC-CO_2, resulting in low or minimal damage to the reservoir and enhanced production.[34,37−39] Therefore, SC-CO_2-based fracturing has emerged as a critical option, for extracting additional hydrocarbons through increased fracture creation. Moreover, with preferential adsorption of CO_2 and desorption of CH_4, SC-CO_2-based unconventional-play development can further sequester additional CO_2.[22,34,40,41] In the recent past, the importance of SC-CO_2 has been identified, and, consequently, a lot of research has focused on SC-CO_2 and shale/coal interaction.

Although research on SC-CO_2 interaction with shale has been gaining momentum the past few years, a comprehensive explanation about the change in geochemical, geomechanical, petrophysical, and pore attributes is lacking. Most experimental studies focus on a specific aspect of SC-CO_2−shale interaction and thus, lack the bigger picture. In the case of simulation-based studies, although reservoir scale changes in shale properties are considered, such approaches lack experimental validation. This study attempts to summarize findings of research efforts on SC-CO_2−shale interaction and provide critical insights on the shortcomings of current approach and future scope of research in this domain. Implementing interdisciplinary approaches and amalgamation of experimental and simulation techniques will enhance the understanding and thereby expedite commercial-scale CO_2 storage operation through enhanced gas recovery in shales.

https://doi.org/10.1021/acs.energyfuels.2c01894
Energy Fuels 2022, 36, 9882−9903

2. PROBLEMS WITH HYDRAULIC FRACKING

To economically produce hydrocarbons from the "difficult to develop" low-permeability horizons such as shale, advanced technologies such as horizontal drilling and multistage hydraulic fracturing has played a significant role.[42−45] In comparison to conventional wells where only a vertical hole is drilled, for unconventional reservoir development first, a vertical well is drilled to typically depths of 1500−3500 ft, followed by horizontal drilling from that depth from distances up to several thousands of feet.[43] Hydraulic fracturing is induced by forcing great volumes of "propping" agent bearing fracking fluids at high pressures, which creates fracture within the target horizon. Once the fractures are created, the hydrocarbons (gas and oil) desorb (due to lowering of pressure), and they flow out and are collected at the vertical wells.[43]

Although successful and has revolutionized the international energy landscape, exploitation of shale resources and the technique of hydraulic fracking has drawn severe concerns and criticisms for its impact on several environmental fronts. An intense debate and concern among the public has been triggered regarding the possible environmental and human health implications and effects that are being caused or likely to be caused due to the rapid expansion, development and extraction of this unconventional energy.[46] Some primary concerns include groundwater and surface water contamination, air pollution, greenhouse gas emissions, and radiations.[4,46−56] Possible contamination of (a) shallow aquifers with hydrocarbon gases from deeper sources, (b) surface and shallow groundwater from improperly treated shale wastewater, and (c) addition of toxic elements, including radioactive elements, in soils near poorly treated disposal sites or spills, have been identified as possible sources of contamination. The involvement of huge volumes of water for hydraulic fracking has also been a point of serious concern for industry, policy makers, and other stakeholders, particularly for water-scarce areas.[43,46,57] It has been documented that deleterious products may be formed due to the interactions between the chemicals present in the injected fluid and the organic matter, radioactive elements within shales, and some part of these eventually flows back to the surface, and during the journey may contaminate water resources at shallower levels.[50,58,59] Chemistry of flowback water and produced water helps in understanding the degree of contamination that occurs due to the impact of hydraulic fracturing.[46] Generation and addition of CH_4, CO_2, and other volatile organic chemicals (VOCs) to air from shale hydrocarbon handling plants and trucks has been cited for causing air pollution around the Marcellus Shale boom.[47]

In addition to issues pertaining to those mentioned above, fracking-induced seismicity has also been raised to be a point of serious concern, which can potentially impact the integrity of surface structures, subsurface infrastructure and wellbore stability.[46,51,60−62]

In addition to the use of large volumes of water, possible contamination of the same and shallower groundwater sources, application of water-based fracking techniques has also been identified to be detrimental toward continued hydrocarbon recovery from shale reservoirs. Specific clay minerals in shales can take up substantial amounts of water in their structures during shale−water interactions, resulting in their volumetric expansion, and subsequently results in closure of pre-existing and created fractures. This self-annealing feature of shales owing to presence of mixed layer clays, results in reduction of permeability and flowage of hydrocarbons. With increasing water saturation, permeability of clay-rich shales decreases.[63−67] With the view of tackling the above-mentioned problems, in recent years, nonaqueous based fracturing using CO_2 (see section 4) has emerged as a better alternative to water-based fracturing while presenting immense possibility of increasing carbon neutrality and achieving negative GHG emissions through geological sequestration.[22,40,68−71] Before the fracturing process, SC-CO_2 can also be used as drilling fluid (see section 3) and has several advantages over other water-based fluids in formations where achieving underbalanced condition near the bottom hole becomes necessary in order to avoid formation damage.[72]

3. SC-CO_2-BASED DRILLING

Traditionally, water-based fluids were used for drilling tight gas reservoirs for the recovery of oil and gas resources.[40,73] However, unconventional reservoirs vulnerable to formation damages are not ideal to drill with water-jets because it can cause excessive overbalance condition near the bottom hole, resulting from the hydrostatic pressure exerted by the produced mud.[74] In such a scenario, underbalanced drilling (UBD) is helpful because, in place of heavy drilling fluids and muds, a light mineral oil,[75] nitrogen foam,[76] and sometimes compressed air[77] are used to achieve underbalanced well conditions and the low density of such drilling fluids will cause the hydrostatic pressure in the wellbore to be lower than the internal fluid pressure of that formation, resulting in the production of reservoir fluids while drilling.[78] However, the density of these fluids is not sufficient enough to generate enough torque for the bottom-hole motors to rotate at its maximum efficiency.[79] Fortuitously, SC-CO_2, because of its liquidlike density, is able to provide sufficient power to rotate the down-hole motor. Moreover, the low viscosity of SC-CO_2, compared to conventional drilling fluids, help in lowering the frictional head loss.[80]

SC-CO_2 drilling, because of its above-mentioned special physical properties, can achieve higher rates of penetration and lower threshold pressure, thus enabling it to have incomparable technical advantages over other drillings techniques.[74] Typical SC-CO_2-based drilling process involves storage of liquid CO_2 in a high-pressure tank.[81] A high-pressure pump is used to pump liquid CO_2 to the bottom hole. At deeper depths, when the pressure and temperature in the underground environment exceeds the critical ones, the CO_2 transfers to a supercritical state. Obviously, different geological basins will have different geothermal and pressure gradients, so the depth at which CO_2 would attain the supercritical state will vary. The SC-CO_2 fluid passes through the drill bit generating SC-CO_2 jet. The drilling is followed by SC-CO_2-based fracturing (see section 4). The SC-CO_2 fluid can then be sequestered into the reservoir either during the fracturing phase or via injection after the depletion of the reservoir.[40]

Initial laboratory experiments compared the penetration depth and threshold pressure of CO_2 with that of water under the same conditions in granite and shale rocks.[72] The results show the penetration depth with CO_2 to be higher than that of water. The threshold erosion pressure was observed to be less than half that of water in shale and two-thirds that of water in granite. Moreover, as explained earlier, when water-based drilling fluids were used to exploit unconventional shale reservoirs, an overbalanced condition occurs at the bottom hole. This pressure difference causes the solid particles in drilling fluids (barite and clay) to enter easily into the formations, thus

https://doi.org/10.1021/acs.energyfuels.2c01894
Energy Fuels 2022, 36, 9882−9903

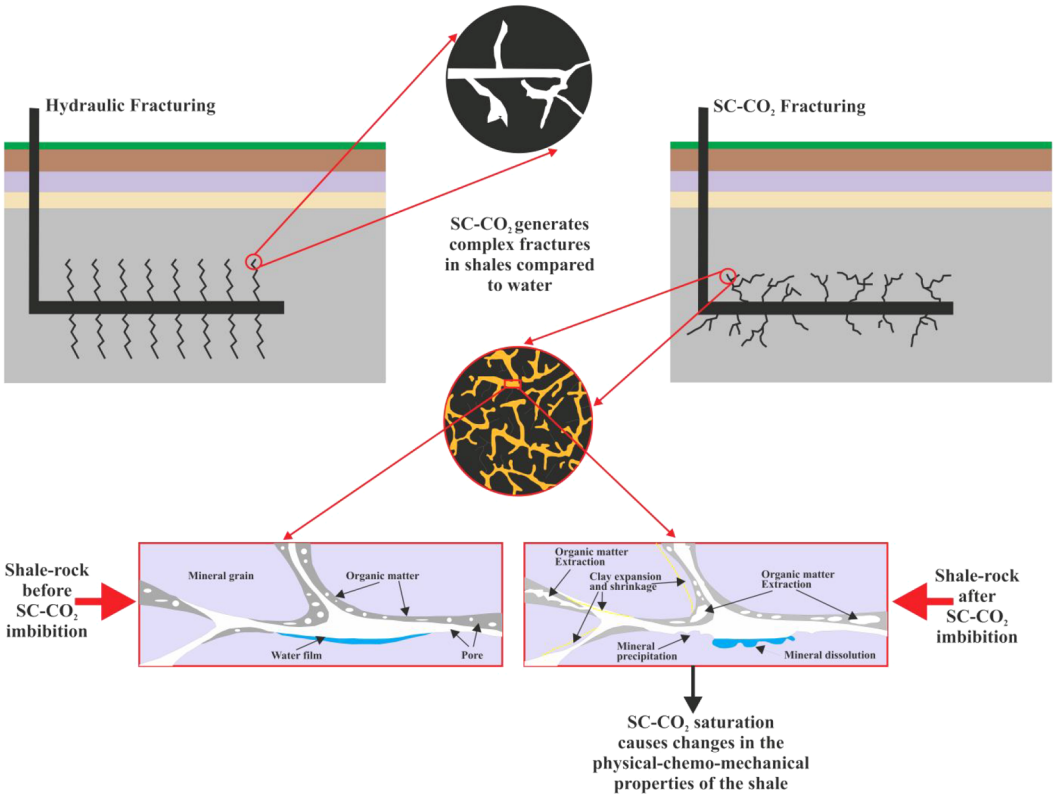

Figure 2. Advantages of SC-CO_2-based fracturing over hydraulic fracturing and the effect of SC-CO_2 imbibition that brings changes in the physical-chemo-mechanical properties (adapted from Pan et al.[35]).

plugging the pore throats.[82] Also, severe plugging of pore throat can occur due to invasion of mud filtrate into the formation.[83,84] This causes an increase in the gas and oil flow resistance. SC-CO_2 fluid does not pose this problem, since there are no solid particles or liquid in it. SC-CO_2 has some moderate to strong influence on rock mechanical properties as well (see section 6). Consequently, the above-mentioned problems can be mitigated when SC-CO_2 is used as a drilling fluid. Additionally, large density of SC-CO_2 fluids dissolves the organic matter[85] and heavy oil components near the wellbore.[86] To control the dissolving capability, the density of SC-CO_2 can be changed by changing its pressure and temperature.[87] The dissolving capability of SC-CO_2 varies greatly as a function of the substance to be dissolved. It is related to the polarity, boiling point, and molecular weight of the substance.[88] This characteristic of SC-CO_2 helps reduce damage near the wellbore and decreases the skin factor, thereby reducing the oil and gas flow resistance. Haizhu et al.[89] prepared a mathematical model based on the special physical properties (density, viscosity, thermal conductivity, heat capacity, etc.) of supercritical CO_2 to study the influence of formation water invasion on the distribution of temperature and pressure in the wellbore during SC-CO_2 drilling. They found temperature of the wellbore fluid to increase with increasing rate of formation water invasion. The wellbore annulus pressure was also found to be directly proportional to the rate of invasion of formation water. Various other aspects of SC-CO_2-based drilling were analyzed[90,91] to optimize the drilling process for efficient recovery of hydrocarbons from unconventional sources. Long et al.[90] used computational fluid dynamic (CFD) model to simulate the effects of inlet temperature and inlet pressure on the mass flow rate and the impinging SC-CO_2 jet flow characteristics. They observed that a slight increase in the inlet temperature resulted in the reduction of both the mass flow rate and the impact of the carbon dioxide jet, whereas, high inlet pressures resulted in their increase. Huang et al.[91] conducted an experimental study to analyze the rock erosion characteristics (erosion area and depth, erosion intensity evaluated by mass loss, and erosion rate) of self-excited oscillation pulsed SC-CO_2 jet (SOPSJ). They employed a Helmholtz oscillation nozzle to generate SOPSJ. They observed that unlike the continuous jets, for the initial several stand-off distances, the SOPSJ's created erosion areas remained constant and then decreased slowly with the growing standoff distances, while the erosion depths first increased and then decreased. Moreover, SOPSJ's resulted in larger mass losses than the continuous jets.

Despite some clear advantages of SC-CO_2-based drilling over other drilling fluids, it has its own set of problems. Ansaloni et al.[92] reviewed the influence of high-density CO_2 on elastomers that are used within the CO_2 transport process. They learned that liquid-phase CO_2 is a good solvent and by using Hansen solubility parameters, the interaction between polymers and solvents could be accounted. Differences in the solubility parameter below two digits lead to substantial absorption of the solvent into the polymer resulting in significant swelling. Therefore, the high-pressure motor of a CO_2 drilling system requires its sealing element i.e., elastomers (a natural or synthetic polymer, e.g., rubber, typically used as sealing materials in CO_2 drilling system) designed in such a manner that it is compatible with supercritical CO_2.[74] On the other hand, the issue of solids transportation, for example, its poor cuttings carrying ability associated with the low viscosity of SC-CO_2 is a

https://doi.org/10.1021/acs.energyfuels.2c01894
Energy Fuels 2022, 36, 9882−9903

key issue that to a certain extent has hindered its application in the oil and gas industry.[93,94] However, the cuttings carrying ability of supercritical CO_2 can be easily increased using additives such as fluoroether disulfate telechelic ionomer.[34] In addition to this, increasing the density of SC-CO_2 could be helpful in increasing its cutting-carrying ability. Shen et al.[86] built a mathematical model to describe the cuttings-carrying process in the horizontal eccentric annulus with SC-CO_2. On the basis of simulation results, they suggested that by controlling the wellhead back pressure the density of SC-CO_2 can be controlled to meet the requirement of cuttings carrying. SC-CO_2 drilling with its several advantages over other drilling methods is a promising technology that still awaits large-scale field implementation in a wide range of basins all over the world.

4. SC−CO_2-BASED FRACTURING

Fracturing of unconventional rock formations using nonaqueous fluid such as SC-CO_2 has several advantages over fracturing based on aqueous fluids:

(1) Low viscosity and high diffusivity of SC-CO_2 fluid makes it comparatively easier than aqueous fluids to generate complex fracture networks;[95−97]
(2) Sharp alleviation of formation damage due to high flow-back rate and little swelling of clay, in comparison to hydraulic fracturing;[98]
(3) Enhanced production due to its higher adsorption capacity to shale than CH_4, resulting in the displacement of preadsorbed CH_4;[99,100]
(4) Minimizes environmental pollution and saves precious water resources.[38,101,102]

Figure 2 displays the advantages that SC-CO_2-based fracturing has over hydraulic fracturing and how SC-CO_2 saturation brings changes in the physio-chemo-mechanical properties of shales. Zhang et al.[103] conducted the simulation experiment to study SC-CO_2 fracturing in shales. They employed acoustic emission and high-energy CT scanning techniques to monitor the progress of fracturing and its morphology, respectively. Results of CT scanning displayed numerous irregular cracks induced by SC-CO_2 fracturing. These cracks formed complex fracture networks after connecting with the bedding and the natural fractures. The volume of rock fractured by SC-CO_2 fracturing was several times higher than hydraulic fracturing. They also found differences in the magnitude of maximum and minimum horizontal stresses causing changes in the patterns of the main fracture. With low horizontal ground stress differences, the fractures were mainly distributed around the simulated drill hole while connecting with the natural fractures and beddings, whereas the fractures went straight through the bedding plane, forming a single main crack when the stress difference was large. Wang et al.[104] studied the effect of SC-CO_2-based fracturing on Niobrara shale with pre-existing fractures. To induce fractures, they injected SC-CO_2 into the center of the shale samples under triaxial stresses. Results show that SC-CO_2 injection caused instantaneous initiation and propagation of SC-CO_2-induced fractures to the rock boundary. They also observed CO_2 expansion helping alleviate the fluid pressure drop and further promotion of fracture propagation as the required propagation pressure decreased with enlarging fracture size. Wang et al.[105] used simulation models to compare variations in the induced fractures caused by different fracturing fluids (water, oil, and SC-CO_2). The results show SC-CO_2 exhibiting the lowest breakdown pressure (the pressure at which the rock matrix begins to fracture), followed by water and oil. This agrees with the laboratory experiments conducted by Ha et al.[106] on mortar specimens. Moreover, SC-CO_2-induced fracture geometry was observed to have higher tortuosity than those by water and oil. Ishida et al.[107] conducted fracturing experiments on cubic granite specimens using water, viscous oil (viscosity of 0.051−336.6 mPa.s), SC-CO_2, and liquid CO_2 as fracturing fluids in order to investigate how fluid viscosity affects the hydraulic fracturing process and crack properties. The results demonstrated the fracturing fluid with the lowest viscosity, in this case, SC-CO_2 had the lowest breakdown pressure, compared to others. Extensive three-dimensional (3D) cracking was induced by low-viscosity fluids while high-viscosity fluids have a tendency to induce two-dimensional (2D) cracks. Moreover, fractures induced by low-viscosity fluids were shear-dominated fractures, whereas the ones induced by viscous fluids were tensile-dominant. The success or failure of fracturing is dependent on the stimulated reservoir volume (SRV). Bennour et al.[108] used three different fracturing fluids with different viscosity (oil, water, and liquid CO_2) to induce fractures in shale and granite samples, so that the variations in the resulted SRV can be studied. The results show the fracturing fluid with lowest viscosity (liquid CO_2) would be capable of achieving more productive fracture network with better SRV. However, the low viscosity of SC-CO_2 does not work in its favor when its proppant carrying capacity is compared with the water-based fracturing fluids.[109] Proppants are vital to the fracturing process because they are required to keep the created fractures open after removal of the injection pressure in order to avoid reclosure due to high overburden pressure.[110] Although the SRV created by SC-CO_2 fracturing are larger than the water-based fracturing fluids, the transport of proppant into the created fractures is severely limited when opted for SC-CO_2 fracturing. Zhang et al.[111] reviewed that, apart from viscosity, the proppant carrying capacity is also dependent on the flow velocity of the fracturing fluid. Increasing the flow velocity alters the flow phase from laminar flow to turbulence flow. Under these conditions, fluid viscosity has almost no influence on the drag force. Therefore, it is suggested that during SC-CO_2 fracturing enough proppants can be carried into the created fractures if higher pump rates are used. However, the velocity of the fluid decreases when it reaches the far end of the fractures. This decrease in velocity again changes the flow phase from turbulent flow to laminar flow restricting proppant distribution at the far end of the fractures. The uncertainty over distribution of proppants using SC-CO_2 and the closure of narrow unpropped fracture apertures due to high effective closure stresses results in the wastage of the comparatively greater SRV created by SC-CO_2. Therefore, Ahn et al.,[112] in their study, regarded the Propped Stimulated Reservoir Volume (PSRV) as the original or effective volume of the reservoir. Microproppants with high portability enhance proppant concentrations at far ends of the fracture network created by SC-CO_2 fracturing which helps in narrowing down the difference between SRV and PSRV. The high portability of microproppants makes it susceptible to form multilayers.[111] A protective layer is formed by the outermost proppant layer against proppant embedment for inner layers. More importantly, proppant embedment is reduced due to lower stress concentration between microproppants and fracture surfaces of shale. Microproppants prevent the closure of fracture under high stress due to higher crushing resistance, thanks to the presence of fewer internal defects.[113] With all its advantages, the use of microproppants during SC-CO_2 still lacks wide-scale field

https://doi.org/10.1021/acs.energyfuels.2c01894
Energy Fuels 2022, 36, 9882−9903

Table 1. Factors Influencing SC-CO_2 Fracturing on the Basis of Breakdown Pressure

fracturing fluid	influencing parameters	breakdown pressure, B_p (MPa)	major observations	reference(s)
			Viscosity (mPa s)	
SC-CO_2	0.051	9.10	the lower viscosity of SC-CO_2 fluid resulted in lowest breakdown pressure helping in easier fracture propagation, compared to other fracturing fluids	Ishida et al.[107]
liquid CO_2	0.097	11.96		
water	0.774	12.96		
oil	316.0	23.07		
			Viscosity (mPa s)	
liquid CO_2	0.10	6.81	fluid with lowest viscosity used for HF of shale reservoirs can achieve more productive fracture network with better SRV	Bennour et al.[108]
water	1.00	8.86		
oil	270.00	16.44		
			Dynamic Viscosity ($\mu_{\text{fracturing fluid}}$/Pa s)	
SC-CO_2	4.04×10^{-5}	8.44	dynamic viscosity of SC-CO_2 has a similar effect as static viscosity, resulting in better fracture network formation	Wang et al.[105]
water	0.79×10^{-3}	12.8		
oil	316.8×10^{-3}	13.0		
			Perforation Angle (deg)	
SC-CO_2	0	12.89	perforation angle has significant effect on the fracture propagation in shales; compared to water, SC-CO_2 fracturing was observed to be better than SC-CO_2 for fracturing through different perforation angles	Chen et al.[98]
	30	13.21		
	45	15.38		
	60	16.03		
	90	16.27		
water	0	14.5		
	30	14.27		
	45	14.07		
	60	16.81		
	90	18.01		
SC-CO_2	25	20.21	SC-CO_2 becomes less viscous with increasing temperature, resulting in easier fracture propagation due to lower breakdown pressure	Zhou et al.[120]
	40	17.82		
	55	16.78		
	70	16.53		
	85	13.36		
	100	13.24		
			Bedding Plane Angle (deg)	
SC-CO_2	0	40.51	fracturing with SC-CO_2 becomes easier with increasing bedding plane angle; this is consistent with the observations made by He et al. 2018, who found that fracturing with both SC-CO_2 and freshwater became easier with increasing orientation angle, but the B_p value of samples fractured with freshwater was higher than those fractured using SC-CO_2	Zhang et al.[122]
	15	36.38		
	30	34.42		
	45	35.89		
	60	32.31		
	75	34.49		
	90	31.09		
			Injection Rate (mL/min)	
SC-CO_2	10	55.42	fracture creation becomes difficult with increasing fluid injection rate	Jia et al.[123]
	15	52.26		
	20	55.22		

implementation, particularly because of the high cost and potential safety issues involved.

Perforation hole plays an essential role as a channel between the wellbore and reservoir.[114,115] The density and orientation of perforation holes decide the magnitude of the breakdown pressure and has an effect on the complexity of the induced fractures.[116,117] Chen et al.[98] conducted a series of fracturing experiments using SC-CO_2 and water as fracturing fluids to investigate the influence of perforation orientation on fracture initiation and propagation process. They found that (a) for both SC-CO_2 and hydraulic fracturing, breakdown pressure decreased with increasing perforation angle; (b) results of acoustic emission demonstrated magnitude of energy release rate from SC-CO_2 fracturing was 1−2 orders of magnitude higher than that of hydraulic fracturing. Essentially, it indicates that more fractures were induced by SC-CO_2 fracturing than hydraulic fracturing; (c) in SC-CO_2, the fracture initiation and extension followed the direction of maximum principal stress when the perforation angle was <45° and became more and more complex at higher perforation angles (>60°); and (d) the fracture propagation direction had little dependence on the perforation angle. Wang et al.[118] investigated the influence of key parameters, such as jet standoff distance and jet pressure, fluid temperature, and ambient pressure, on the perforation ability of the SC-CO_2 jet. They observed ambient pressure having no substantial effect on perforation under fixed jet differential pressure conditions. Moreover, increasing the confining pressure from 5 MPa to 15 MPa resulted in 5.7% and 18.6%

https://doi.org/10.1021/acs.energyfuels.2c01894
Energy Fuels 2022, 36, 9882−9903

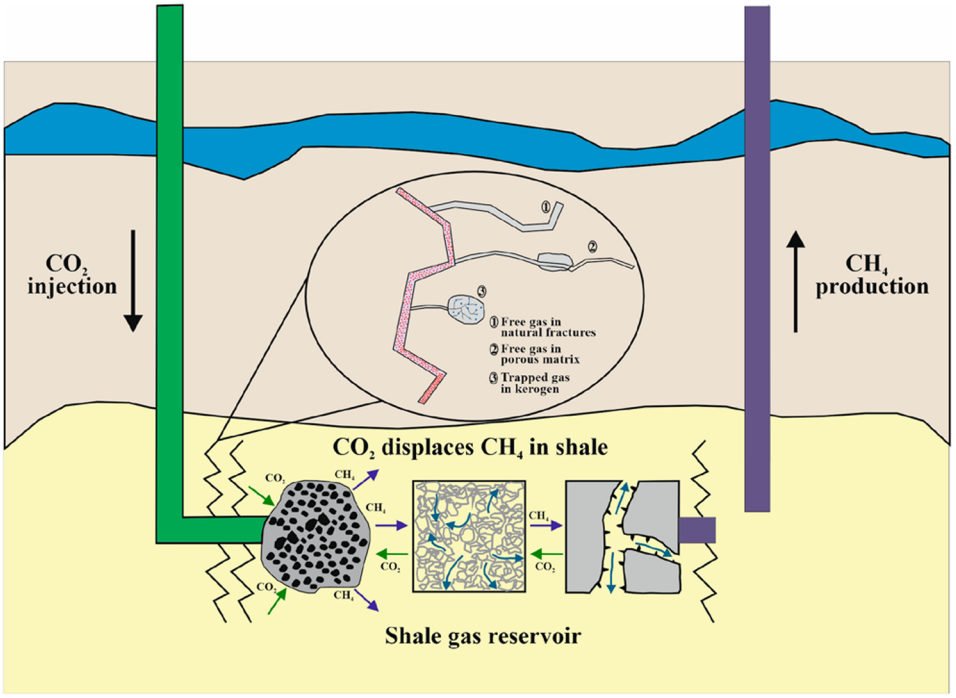

Figure 3. Schematic of three gas place origins of methane and competitive adsorption in shale reservoirs (adapted from Middleton et al.[40] and Godec et al.[127]).

decreases in the hole depth and diameter, respectively. On the other hand, with increasing jet temperature (40−100 °C) and standoff distances (4−10 mm), the hole depths increased by 3.8% and 12.0%, respectively. High temperature lowers the viscosity of SC-CO_2, causing it to permeate easily into the microcrack tip and encourage fracture propagation.[34,119] Zhou et al.[120] studied the effect of temperatures (varying between 25 °C to 100 °C with an interval of 15 °C) on the SC-CO_2 fracturing of artificial specimens. Results demonstrated a linear decrease in the breakdown pressure of SC-CO_2 fracturing with increasing temperatures. At temperatures above 85 °C, the phase change of SC-CO_2 within the fractures promoted branched or crossing fractures around the main fractures resulting in the formation of a fracture network. However, the prediction of the phase change of CO_2 can be a complicated process.[121] Therefore, during liquid CO_2 fracturing, monitoring of pressure changes is very important to get clear idea about the phase change at each stage. Table 1 summarizes various factors influencing SC-CO_2 fracturing on the basis of breakdown pressure.

Field implementation of this fracturing technique is still lacking. Fluid injection can lead to changes in rock stress field and induce microseismicity which, if felt, may result in negative public perception about the project and may also endanger wellbore stability.[124] Therefore, detailed mapping and evaluation of microseismic response after SC-CO_2 fracturing of a range of shale formations is required to evaluate the true potential of the technique in better fracture network development over others.[34] Nevertheless, review of the current literature suggests that SC-CO_2 still faces certain challenges (e.g., poor cuttings carrying ability and proppant carrying capacity) in replacing slick water as the primary drilling and fracturing fluid.

5. CO_2 ADSORPTION VERSUS CH_4 DESORPTION: Vis-à-Vis CO_2 SEQUESTRATION

As already mentioned, one of the advantages of using SC-CO_2 for fracturing shale petroleum systems is the possibility of permanently sequestrating CO_2 in deep shale reservoirs. When injected, CO_2 is preferentially adsorbed over the preadsorbed CH_4, as both mineral matter and organic matter within shales show more affinity toward CO_2 than CH_4.[27,125] In fact, the enhanced recovery of CH_4 and simultaneous sequestration of CO_2 is seen as the first step for CCS to ease the financial burden with CO_2 capturing and handling.[11,126] The fact that CO_2 displaces CH_4 and is adsorbed by shale pores is similar to the process that operates in coal bed methane systems, and has been proved by both experimental studies and numerical simulations.[124,127−129] In addition to displacing the adsorbed CH_4 from porous structures within the shale reservoirs, pre-existing fractures and created fracture networks also provide additional sites for CO_2 adsorption.[27]

Different researchers have simultaneously performed CO_2 and CH_4 adsorption experiments on shales. Weniger et al.[130] observed that CO_2/CH_4 adsorption capacity ratio to vary between 1.9 and 6.9, for Permian and Devonian coals and shales from Brazil. Heller and Zoback[125] observed the volume of CO_2 adsorbed by pure minerals and the U.S. shale samples to be 2−3 times higher than the volume of CH_4 adsorbed. Chareonsuppanimit et al.,[131] on their work on New Albany shales, observed CO_2 adsorption capacities to be several times higher than the CH_4 adsorption capacity. Results from these and several other studies[24,132,133] show the influence of total organic carbon (TOC) content on gas adsorption capacity of shales, as gas in shale reservoirs are primarily stored through adsorption on the organic matter pores.[24,134] In another work on Woodford and Caney shale plays, Chareonsuppanimit et al.[135] observed that, at ~7 MPa, the adsorption ratio of N_2, CH_4, and CO_2 to be 1:(2.9−3.5):(6.1−30.1), with the CO_2 preferential adsorption over CH_4

https://doi.org/10.1021/acs.energyfuels.2c01894
Energy Fuels 2022, 36, 9882−9903

being stronger for high ash shales, indicating the important role of mineral matter on gas adsorption. Gasparik et al.[136] observed low-TOC Palaeozoic and Mesozoic shales from The Netherlands to have higher sorption capacities than high-TOC shales, with the sorption capacity being correlated with clay contents. Hazra et al.,[137] in their work on Permian shales from India, observed positive role of clay minerals on CH_4 sorption capacity, although TOCs were observed to principally control gas storage capacity.

Competitive adsorption of CO_2 in place of CH_4 is fundamentally related to the sizes of CO_2 and CH_4 molecules,[138−140] and also the molecular weights of the gases. CO_2, because of its smaller dynamic diameter of 0.33 nm, accesses finer pores and narrower pore areas, in comparison to CH_4(molecular diameter of 0.38 nm). Consequently, when CO_2 is injected, a volumetric sweep is achieved, by removal of CH_4 and adsorption of CO_2 in place. Figure 3 shows three gas place origins of methane and competitive adsorption in shale reservoirs. SC-CO_2, because of its liquid-like density and capacity to access greater organic nanopore areas, can displace greater amounts of CH_4. Simultaneously greater volumes of CO_2 can be sequestered within shale horizons, as the SC-CO_2 has access to greater amounts of sorption sites.[140]

Among different properties viz. temperature,[141] moisture content,[133] the role of organics in shale reservoirs is of primary significance, as the organic matter primarily stores the hydrocarbons and similarly their role in storing the CO_2 is primary. Kerogen within shales, depending on the type and thermal maturity level, can show development of nanoporous structures, which offers high surface areas and thereby adsorbs huge volume of gas.[7,32] The large hydrocarbon storage capacity of kerogen within shales makes them interesting targets for CO_2 sequestration. Different researches have documented the strong role of TOC and thermal maturityon CH_4 and CO_2 sorption capacity of shales (see Wood and Hazra,[7] and references within). Organic-hosted porosity is one of the most critical elements in successful shale plays. Different techniques viz., imaging (e.g., broad ion beam-scanning electron microscopy, and focused ion beam-scanning electron microscopy), gas adsorption (low pressure and high pressure gas adsorption techniques), mercury intrusion porosimetry, neutron scattering (e.g., ultrasmall/small angle neutron scattering), etc., are used to assess shale porosity.[7,24,32,142−163] In addition to several factors, such as the presence of surface functional groups, the mesopores and micropores, and the specific surface area, etc., thermal maturity levels have been identified to strongly control the development of organic porosity and, hence, the gas adsorption capacity of shales and carbonaceous matter.[164−167] Loucks et al.[167] observed organic nanopore development to be strongly dependent on the thermal maturity levels of the samples and inferred that this is essentially caused by the conversion of kerogen to hydrocarbons and the formation of pores within the organic matter in the process.

The type of kerogen also strongly influences the gas adsorption capacity of shales. Zhang et al.[168] observed small but systematic differences in the sorption capacity of U.S. shales, with type III kerogen-bearing shales showing highest sorption capacity followed by type II and type I shales. They related this with the inherently higher aromaticity of type III kerogen. Hazra et al.[137] observed CH_4 adsorption capacity of vitrinite (type III kerogen)-rich Permian shales from India to be higher than those shown by inertinite (type IV kerogen)-rich shales. The presence of reactive or inert organic matter in shales, and their corresponding response to thermal maturation, controls the porosity development and gas adsorption capacity of shales. Loucks et al.[167] documented that, for reactive organic matter, with progressive thermal maturation, pores are formed as hydrocarbons are released. On the other hand, for nonreactive organic matter (type IV kerogen), because of their inherently lower hydrocarbon generation capacity, little or insignificant changes in organic porosity is observed with maturity enhancement.[167]

Generally, laboratory experimental data generated by several researchers clearly demonstrate that, with increasing pressure, CH_4 adsorption capacity increases monotonously, and then reaches a more or less constant value at higher pressures (see Klewiah et al.[140] and references within). A similar response is also seen when CO_2 is used as the adsorbate, but only until the pressures of up to supercritical transition point. At the supercritical state, the CO_2 adsorption amount reaches maxima, and thereafter reduces systematically. Obviously, this supercritical transition point is dependent on the temperature at which the laboratory experiments are conducted. For example, Weniger et al.[130] observed the CO_2 adsorption maxima and thereafter reduction on Permian and Devonian coals and shales from Brazil between 8 and 10 MPa, when the adsorption experiments were performed at 45 °C. On the other hand, Merey and Sinayuc[169] observed the similar maxima and subsequent reduction on shales from Dadas Formation, Turkey, at 6.43 MPa at 25 °C. Figure 4 shows the CO_2 vs CH_4 excess sorption as a function of pressure for a high-TOC shale from Irati Formation, Brazil.[130] The supercritical behavior of CO_2 at higher pressure render the Langmuir theory to be inapplicable, and, instead, other models, viz. the Ono-Kondo monolayer and three layer models for laboratory measurements.[169] Langmuir model generally is more appropriate for low-pressure systems, and presents limitations at higher pressures, especially due to the unusual behavior of CO_2 at higher pressures.[130,169] On the other hand, the Ono-Kondo model has been observed to be particularly useful in determining the volume of gas adsorbed from the experimental data, which is generally overlooked when using the Langmuir model.[169]

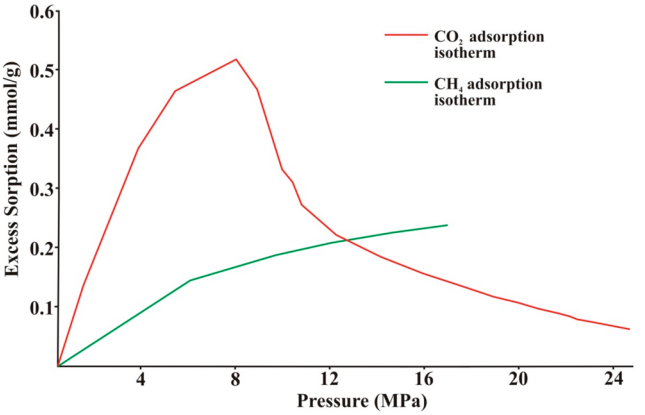

Figure 4. CO_2 vs CH_4 excess sorption, as a function of pressure for a high-TOC shale from Irati Formation, Brazil (redrawn and adapted from Weniger et al.[130]).

https://doi.org/10.1021/acs.energyfuels.2c01894
Energy Fuels 2022, 36, 9882−9903

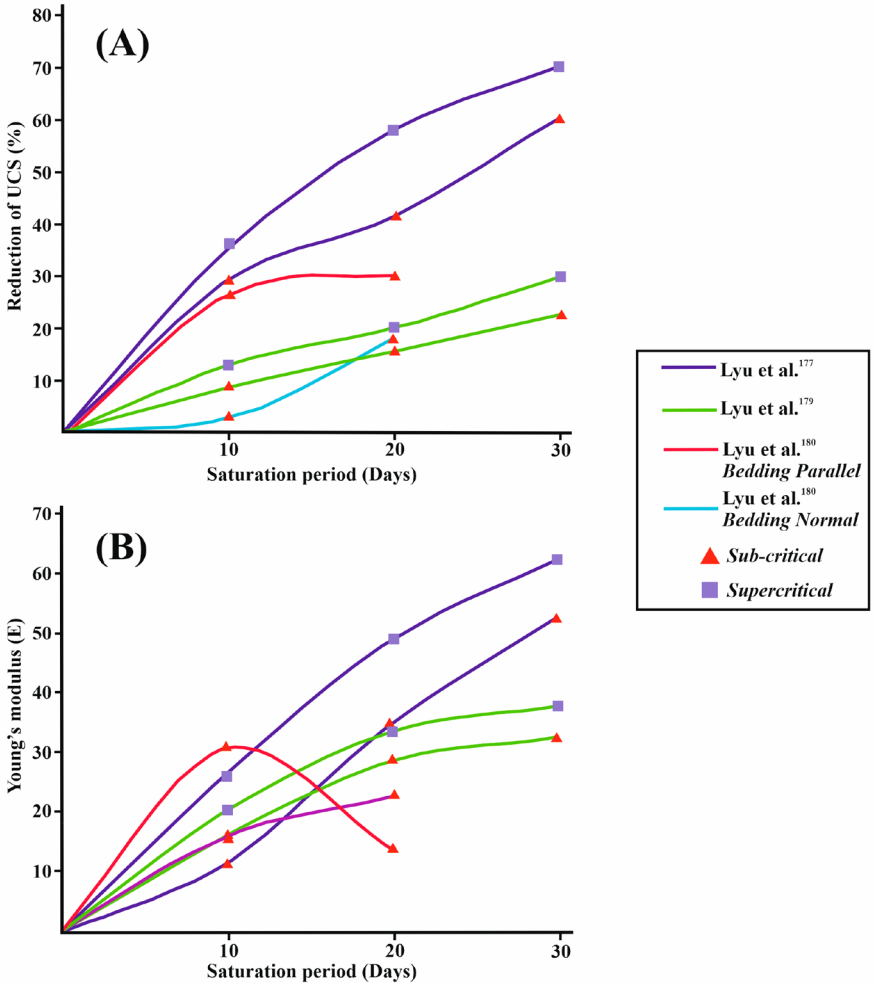

Figure 5. Reduction of (A) uniaxial compressive strength (UCS) and (B) elastic modulus (E) after saturation in subcritical and supercritical CO_2.

6. INFLUENCE OF SC-CO_2 ON SHALE PETROPHYSICS, GEOMECHANICS, AND WETTABLILITY

After SC-CO_2 injection, the interaction between the formation rock and the adsorbed CO_2 intensifies over time bringing changes in the strength properties of the host rock.[170−172] This, in turn, affects the wellbore stability, fracturing efficiency, and geological storage.[173] On the other hand, accurate evaluation of the mechanical properties of the formation can enable successful implementation, as well as optimization of drilling, completion, and hydraulic fracturing in shale reservoirs.[174] Several researchers have examined this issue.[175−178] The studies primarily involved the immersion of rock samples in SC-CO_2 for a certain time period to examine the variations in the strength properties after CO_2 saturation. It has been observed that the tensile strength, triaxial compressive strength, and elastic modulus (E) of shales decreased after SC-CO_2 imbibition. Yin et al.[175] conducted laboratory experiments to study the impact of subcritical CO_2 (sub-CO_2) and SC-CO_2 imbibition on the mechanical properties of organic-rich shales. They observed CO_2 saturation caused loss of strength in shale due to microscopic damages. The extent of the damage was related to the phase-state and gas pressure of CO_2. Sub-CO_2 saturation (gas pressures of 4 and 6 MPa) caused reductions in the uniaxial compressive strength (UCS) and E of the samples, by 22.86% and 23.10%, respectively. On the other hand, SC-CO_2 saturation (gas pressures of 8, 12, and 16 MPa) at 33.89% for UCS and 33.97% for E caused more significant reduction than sub-CO_2 saturation. Moreover, the results demonstrated a slight increase in the mechanical parameters over a pressure range of 12−16 MPa, primarily because of the compression effect due to higher pressure of the fluid. Similar observations from the previous studies are displayed in Figure 5. Zou et al.[176] investigated the impact of CO_2−brine−rock reactions on the petrophysical and mechanical properties of shales. They observed that mineral dissolutions during static soaking experiment caused up to a 1-order-of-magnitude increase in the permeability and porosity, and decreases of up to 71.3% and 9.8% in tensile strength and surface friction coefficient of the shale samples, respectively. Apart from this, saturation time has great impact on the mechanical properties.[181,182] Table 2 provides the summary of the observed changes in the mechanical properties of shales with respect to SC-CO_2 treatment time.

Lyu et al.[179] conducted UCS experiments on shale samples with low clay constituent immersed in (sub-CO_2) and SC-CO_2 fluids for variable time periods. They employed acoustic emission (AE) and scanning electron microscopy (SEM) to understand effect of adsorption time on microscale variations and crack propagation, respectively. The results show the following:

(1) From 10 day imbibition to 30 day imbibition, UCS and E of sub-CO_2/SC-CO_2 saturated samples demonstrated

https://doi.org/10.1021/acs.energyfuels.2c01894
Energy Fuels 2022, 36, 9882−9903

Table 2. Summary of the Effect of SC-CO_2 Treatment Time on the Mechanical Properties of Shales

sampling area	original mineralogical composition before exposure to SC-CO_2[a]	TOC (%)	treatment time	maximum reduction in strength properties (% reduced) with respect to SC-CO_2treatment time[b] (h)		notable changes in mineralogy after SC-CO_2treatment	literature
Black shales, Southeast Chongqing, China	Qtz > F > muscovite > C > pyrite > smectite > illite> annite > kaolinite > braunite	2−4	10, 20, and 30 days	UCS	66.05% after 30 days	EDS analysis showed increase in the percentage of C and Fe and decrease of K and Al	Lyu et al.[180]
				E	56.32% after 30 days		
Longmaxi Formation, Sichuan Basin, China	Qtz > F > P > C> D > pyrite > clay	7.88	24, 48, 72, 96, and 120 h	TS	27.7% after 96 h	quartz content increased after 96 h; mineral content of all other shale minerals decreased as the treatment time increased	Ao et al.[181]
				TCS	15.3% after 120 h		
				E	29.56% after 120 h		
Silurian Longmaxi Formation, Schuan Basin, China	Qtz > D > C > F > clay	3.7	10 days	UCS	28.67% after 10 days	no significant change in mineral content was observed	Yin et al.[175]
				E	31.49% after 10 days		
Changing region, Sichuan basin, China	Qtz > C > G > I > D	3.8	10, 30, and 60 days	TS	46% after 60 days	the study did not consider changes in mineral content	Feng et al.[184]
				E	22% after 60 days		
Sichuan Basin, China	Qtz > F > cristobalite > kaolinite > illite		10, 20, and 30 days	UCS	29.95% after 30 days	carbon content increased after CO_2 adsorption	Lyu et al.[179]
				E	37.79% after 30 days		
Silurian Longmaxi Formation, Chongqing, Sichuan Basin, China	Qtz > D > C > clay > F > pyrite > hematite	–	10 days	TS	11.9% after 10 days	mineral content of all shale minerals decreased after SC-CO₂ treatment except quartz; dissolution of calcite caused the decrease in tensile strength	Lu et al.[185]
				E	5.7% after 10 days		
Longmaxi shale, Sichuan basin, China	Qtz > F > P > C > D > pyrite > clay	7.8	48 h	H	29.5% after 48 h	little to no effect on quartz content; mineral dissolution effect on clay minerals	Shi et al.[186]
				E	11.0% after 48 h		
				FT	11.3% after 48 h		
Songliao basin, China	Qtz > F > Cb > clay > P > siderite	–	3, 7, and 14 days	E	47% after 14 days	quartz content increased by 26% after 14 days; carbonate minerals decreased by 12% after 14 days	Meng et al.[187]
Longmaxi Formation shale, Sichuan Basin, Yibin City, Sichuan Province	brittle minerals > clay minerals > carbonate minerals	3.7	15 and 30 days	TS	57.5% after 30 days	reduction of carbonate and silicate mineral content was observed through EDS analysis	Qin et al.[188]
Silurian Longmaxi Formation, southeast Chongqing, China	Qtz > clay > C > D	–	2 h @ 30 MPa and 335.15 K	UCS	22.9% after 2 h	the study did not consider changes in mineral content	Song et al.[189]
				PR	40.3% after 2 h		

[a]Legend: Qtz, quartz; F, feldspar; D, dolomite; C, calcite; G, Gehlenite; I, illite; Cb, carbonate. [b]Legend: UCS, uniaxial compressive strength; E, elastic modulus; TS, tensile; H, hardness; TSC, triaxial compressive strength; PR, Poisson's ratio; FT, fracture toughness.

https://doi.org/10.1021/acs.energyfuels.2c01894
Energy Fuels 2022, 36, 9882−9903

reductions from 8.79%/12.96% and 16.05%/20.23% to 23.03%/29.95% and 32.61%/37.79%, respectively;

(2) The peak cumulative AE, depicting unstable crack propagation stage, increased as the adsorption time increased;

(3) New pores appeared on the sample surface and an increase in carbon content after sub-CO_2/SC-CO_2 saturation was observed using SEM and energy-dispersive X-ray spectroscopy analysis, respectively.

Zhou et al.[190] conducted similar experiments to evaluate the impact of adsorption time on the permeability and the corresponding stress sensitivity of fractured shale. The results indicated that the stress sensitivity of shale permeability after CO_2 saturation were amplified due to the weakening effect caused by CO_2−shale interaction. Choi et al.,[178] in their experiment consisting of saturation of shale specimens with SC-CO_2 + brine for 63 days, found significant weakening of strength properties of the shale. However, with only SC-CO_2 as a treatment fluid, a self-healing effect was observed, which was caused by the precipitation of secondary sediments, leading to an increase in the strength and elastic properties. Feng et al.[184] evaluated the effect of adsorption periods as well as layer orientations on the strength properties of the shale samples. Results revealed reduction in the Brazilian splitting strength (BSS) and Brazilian splitting modulus (E) of shale samples with increasing adsorption time. Adsorption for 10, 30, and 60 days resulted in the BSS reduction of 11.30%, 40.66%, and 45.68%, compared to the samples without adsorption, respectively. For inclination angle range $0 \leq \theta \leq 45°$, the BSS of the samples increased and for range $45° \leq \theta \leq 90°$, it decreased. The variations in the strength characteristics for samples with different adsorption time revealed similar change trends with the bedding orientation angle. The effect of SC-CO_2 imbibition for 30 days on the triaxial compressive strength of low-clay samples was investigated by Lyu et al.[191] They observed increase in the axial stresses with increasing confining pressures with or without SC-CO_2 saturation. However, axial stresses of samples with the same confining pressure revealed losses in strength and rigidity, because of SC-CO_2 imbibition. Results of cohesion and internal friction angles of the samples treated with or without SC-CO_2 revealed minor differences, indicating the applicability of Mohr−Coulomb criterion in both cases to be valid. Similarly, Ao et al.[183] evaluated the strength properties of shale treated with SC-CO_2. The results demonstrated decrease in the triaxial compressive strength, tensile strength, and E of the samples after SC-CO_2 treatment. Here, also, the weakening effect intensified as the treatment time increased. Based on X-ray diffraction (XRD) analysis, they explained that the changes were due to the enlargement of pore size caused by the dissolution effect of CO_2. According to the results obtained by them, fracturing fluids induced mineral reactions are the primary cause for the loss of rigidity of shales. On the other hand, in a laboratory experiment conducted by Song et al.[189] found that while the elastic modulus of the shale increased by 32.2%, whereas, the Poisson's ratio decreased by 40.3% after SC-CO_2 saturation for 2 h at a temperature of 335.15 K. The increase in E was attributed to the lesser organic content in the shale, compared to the inorganics.

It is known that shales, in terms of mineralogical composition, vary spatially.[192] Therefore, the overall mechanical response of shale will be dependent on the strength properties of the individual mineral phases.[193] Shi et al.[186] conducted nano-indentation tests on shale samples to determine the mechanical strength differences in the clay-rich and quartz-rich areas of shale samples before and after SC-CO_2 imbibition. The results demonstrated substantial decreases in the mechanical strength of clay-rich area, as a consequence of CO_2 adsorption and mineral dissolution, whereas very small change in quartz-rich area was observed due to little effect on quartz caused by CO_2 imbibition.

As SC-CO_2 is capable of penetrating deep into the microstructure of shales and dissolving polar and weakly polar substances, it can bring substantial changes in the microstructures of the shale rock. The important microstructural properties of shales are as follows:

(i) Mineralogical composition: the key mineral constituents of shale rock are clay, quartz, and calcite, but traces of feldspars, carbonates, and pyrite also exist.[24] Characterization of the mineralogical composition of shale is important for distinguishing the clay and nonclay portions as both demonstrate significant differences in morphology and chemical composition.[194] Also, the alteration in the wetting behavior of shale caprock caused by CO_2 sequestration is dependent on the composition of the clay and nonclay portions.[195,196]

(ii) Organic matter: precise evaluation of the composition, thermal maturity, and quantity of organic matter in shale rock is important because it governs the hydrocarbon generation potential of the reservoir.[197,198]

(iii) Porosity: the gas storage capacity of shale rock is determined by its porosity.[196] There are three types of shale porosities: inorganic porosity (due to minerals), organic porosity (due to organic matter), and fracture porosity.[143,160] The shale matrix is mainly composed of micropores (<2 nm in diameter), mesopores (2−50 nm in diameter), and macropores (>50 nm in diameter).[199]

(iv) Permeability: the flow of gas and oil in the shale is determined by its permeability.[196] It plays a critical role, because shales have extremely low permeability (in nanodarcies).[200]

In recent years, some researchers have focused on the same. A comparative study of gaseous CO_2 and SC-CO_2 saturation reported that the effect of adsorption and swelling governs the change in pore attributes during gaseous CO_2 treatment, whereas SC-CO_2 saturation facilitates the dissolution of minerals.[10,11] Generally, SC-CO_2 can induce easy dissolving and extraction of low-molecular-weight substances.[201] Table 3 summarizes observations of different researchers related to pore structural changes caused in shales due to SC-CO_2 exposure. Jiang et al.[201] observed a host of changes induced in shales, in response to exposure to SC-CO_2 under variable time, temperature, and pressure. Using SEM, they observed that, with exposure to SC-CO_2, clay minerals in shales progressively released the "crystal water" and concomitantly became smaller in size, whereas, on the other hand, the organics were dissolved with the primary porous structures and fractures undergoing transformation. New porous structures were formed in place, which they interpreted would increase pore-fracture connectivity. Furthermore, using MIP, they observed both surface area and porosity of the shales to increase with SC-CO_2 exposure time and pressure.

Yin et al.,[95] in their work on Longmaxi shales in China, observed the dissolution and/or removal of organics and some minerals (such as kaolinite, calcite, and montmorillonite). They also observed that specific surface area, pore volume, and fractal

https://doi.org/10.1021/acs.energyfuels.2c01894
Energy Fuels 2022, 36, 9882−9903

Table 3. SC-CO_2-Induced Changes in Shale Pore Structure, Fractal Dimensions, and Mineralogy

literature	formation/area	nature of samples	experimental conditions	major observations
Yin et al.[95]	Longmaxi Formation, Fuling (FL) and Changning (CN) regions, Sichuan Basin, China	TOC content = 2.98−4.18 wt % Ro: 1.97%−2.54%	pressure: 16 MPa, temperature: 40 °C, time: 30 days	• no changes in pore shape • surface area, pore volume, and number of micropores decreased • fractal dimensions were observed to decrease • concentration of organic matter, minerals such as montmorillonite, kaolinite, and calcite were observed to decrease
Meng et al.[187]	Cretaceous shales, Songliao Basin, China	depth: 2000−3000 m porosity: 4.6%−5.3% permeability: 0.003−0.006 md	pressure: 25 MPa, temperature: 60 °C, time: 0, 3, 7, and 14 days	• carbonate concentration significantly decreases with time • development of honeycomb pores on shale surfaces • increase in low-pressure N_2 gas adsorption capacity, mesopore and micropore volume, with increasing exposure to SC-CO_2
Fatah et al.[225]	Eagle Ford and Mancos shales, United States	Eagle Ford shales − clay-rich, average TOC content — 3.43 wt % Mancos shales- quartz rich, average TOC content = 3.2%	pressure: 18 MPa, temperature: 70 °C, time: 30 days	• increase in quartz content, but decrease in clay and carbonate contents after exposure • with SC-CO_2 exposure, low-pressure N_2 gas-adsorption-derived surface area and total pore volume decreased considerably for the Eagle Ford shale reduced, while the same were observed to increase considerably for the Mancos shale • fractal dimension, D1 was observed to decrease for both the shales • fractal dimension, D2 was observed to marginally increase for both the shales
Fatah et al.[97]	Eagle Ford and Mancos shales, United States	Eagle Ford shales — clay-rich, average TOC content = 3.43 wt % (Rahman et al., 2017) Mancos shales — quartz-rich, average TOC content = 3.2% (Torsæter et al., 2012)	pressure: 18 MPa, temperature: 70 °C, time: 30 days	• increase in quartz content, but decrease in clay and carbonate contents after exposure • surface wettability of clay-rich Eagle Ford shales evolved to CO_2-wet from water-wet with SC-CO_2 exposure, whereas for quartz-rich Mancos shales, wettability stayed water-wet even after SC-CO_2 exposure. • FTIR studies revealed that aliphatic hydrocarbons underwent strong change with SC-CO_2 treatment, while aromatic hydrocarbons showed minimal changes
Pan et al.[202]	two shales from marine Wufeng and Longmaxi Formations China; two shales from terrestrial Chang-7 and Chang-9 member of the Yanchang Formation, China	marine shales: TOC content = 2.05−4.02 wt %, Ro = 2.13%−2.42%; terrestrial shales: TOC content = 4.32−5.64 wt %, Ro = 0.86%−0.92%	pressure: 20 MPa, temperature: 80 °C, time: 14 days	• decrease in quartz, feldspar, and calcite contents with exposure to SC-CO_2, while increase in clay mineral concentration was observed • volume of low-pressure N_2 gas adsorbed, BET SSA, BJH pore volume were observed to decrease for the marine shales and increase for the terrestrial shales with exposure to SC-CO_2 • fractal dimensions, D1 and D2 were observed to decrease with exposure to SC-CO_2 for the marine shales, while the same were observed to increase for the terrestrial shales • similarly, micropore surface area and volume from low-pressure CO_2 gas adsorption, were observed to decrease for the marine shales and increase for the terrestrial shales, with exposure to SC-CO_2
Dai et al.[203]	Longmaxi Formation, China	TOC content = 1.44−4.92 wt %; Ro: 2.00−2.90%	pressure: 8 MPa, temperature: 50 °C, time: 48 h	• feldspar, calcite, and clay were observed to decrease due to exposure to SC-CO_2, whereas quartz was observed to increase • micropore and mesopore volumes and surface areas were observed to increase with exposure to SC-CO_2; moreover, TOC content was observed to play a role in the behavior of the shales.
Ozotta et al.[204]	Upper Bakken (UB) and Lower Bakken (LB) shales	TOC content = 13.3 wt % (UB), 14.4 wt % (LB); T_{max}: 449 °C (UB), 448 °C (LB)	pressure: 7.03 MPa, temperature: room temperature, time: 3, 8, 16, 30, and 60 days	• quartz content increased in the UB shale, while decreased in the LB shales with increasing exposure (days) to SC-CO_2

https://doi.org/10.1021/acs.energyfuels.2c01894
Energy Fuels 2022, 36, 9882−9903

Table 3. continued

literature	formation/area	nature of samples	experimental conditions	major observations
				• the SSA and fractal dimensions of the shales initially increased until 8 and 16 days, and then showed a decreasing trend

dimensions decreased with the increasing exposure to SC-CO_2, while the average pore dimension increased. In their study, however, the variation in TOC (2.98−4.18 wt %) and thermal maturity (all samples overmature; Ro = 1.97−2.54%) of the shales were minimal. Interestingly, using low-pressure N_2 gas adsorption, they did not observe any significant changes in the pore morphology of shales after SC-CO_2 exposure, which contradicts the findings of Sanguinito et al.,[205] where the authors reported changes in pore morphology that were due to etching on the pore surface through cyclic dissolution and precipitation of carbonates. They attributed this change to the effect of dissolution and CO_2-induced swelling behavior. Similar observation was reported in studies conducted by several researchers,[183,206,207] where they also inferred that the change in pore volume due to swelling and dissolution also causes reductions in the mechanical properties of shale and the extent of change is proportional to the time of SC-CO_2 saturation. A detailed investigation of elemental mobility in shales post-SC-CO_2 and water treatment[208] reveals that the primary dissolution happens in the carbonates, mobilizing Ca and Mg elements, whereas the secondary preference is given to clay minerals, mobilizing Na, K, and Al elements. Contrary to previous studies, they reported a minor change in pore morphology, inferred through the change in hysteresis behavior of N_2 LPGA isotherms. Meng et al.,[187] although focused on SC-CO_2-induced geomechanical changes in shales from Songliao Basin, China, noted that the mineral matter content, especially calcite, strongly decreased, because of dissolution, with increasing exposure to SC-CO_2. Similar to other researches, they observed the primary porous structures and fractures to be dissolved and replaced by newer structures formed because of exposure. On the other hand, in another work, Ozotta et al.[204] observed the quartz content to increase in Upper Bakken shales and decrease in Lower Bakken shales , because of shale−SC-CO_2 interaction, while all minerals decreased in content in both the formations. Interestingly, time of exposure showed a very strong influence in their work. The specific surface area and fractal dimensions of the shales initially increased until 8 and 16 days, and then showed a decreasing trend, while the overall pore volume displayed a decreasing trend. For Middle Bakken shales, Wang et al.[209] observed that the mesopores were largely impacted, because of SC-CO_2 exposure, while the micropores and macropores did not show changes with SC-CO_2 exposure. Hui et al.[210] observed variable results for Sichuan and Ordos Basin shales. For the oil-window mature shale (TOC > 5 wt %), they observed a marginal increase in low-pressure N_2-gas-adsorption-derived specific surface area, while a substantial increase was observed in CO_2-derived micropore surface area. In contrast, for the overmature shales, they noted a decrease in both N_2 and CO_2 surface areas with exposure to SC-CO_2. In their research, they noted little or no changes in the mineralogy of the shales with exposure to SC-CO_2. It is also noteworthy to mention that the effect of SC-CO_2 saturation alone on shale pores is completely different from the combined effect of SC-CO_2 and brine. The presence of CO_2 in brine changes the pH of the solution, resulting in HCO_3^- formation, facilitating the deposition of kaolinite, gypsum, amorphous globule,[211] and dissolution of feldspars. The combined effect of such chemical alterations results in almost a 4% increase in porosity, whereas dry SC-CO_2 treatment can cause up to 20% reduction in total pore volume and 36% reduction in surface area.[212]

The surface wettability of shales (and any other reservoir) is another important petrophysical property that is influenced by

https://doi.org/10.1021/acs.energyfuels.2c01894
Energy Fuels 2022, 36, 9882−9903

$SC\text{-}CO_2$ and affects the overall performance of the reservoir, especially for sequestration.[195,214−220] The capillary forces, which are crucial for the evaluation of storage potential, are mainly controlled by surface wettability.[219] Qin et al.[87] conducted laboratory experiments to determine the influence of $SC\text{-}CO_2$ on shale water wettability. They found that the water wettability of shale decreased after $SC\text{-}CO_2$ treatment, resulting in increased diffusion of CO_2 into the shale matrix, which ultimately favors the CO_2 adsorption and CH_4 desorption capacity of the shale. Kaveh et al.[221] in their study evaluating CO_2 wettability of silty shale caprocks found that the contact angle between CO_2 and silty shale was low, indicating a strong water-wet caprock system, making it favorable for CO_2 storage. Fatah et al.[222] evaluated the wettability of two mineralogically distinct shales after $SC\text{-}CO_2$ treatment. The results obtained indicate that the shale/water contact angle alteration was mineralogy-dependent. The clay-rich shales were observed to have transitioned to being CO_2-wet, compared to the quartz-rich shales, which remained strongly water-wet after $SC\text{-}CO_2$ treatment. In a different study conducted by Fatah et al.,[223] they compared the shale/water contact angles of three type of shales (Eagle Ford, Wolfcamp, and Mancos) with various mineralogy exposed to $SC\text{-}CO_2$ at different durations, pressures, and temperatures. They observed that, for clay-rich shales (Eagle Ford and Wolfcamp), the CO_2/shale contact angle continuously increased with increasing treatment time and pressure, caused by dissolution of clay and carbonate minerals, whereas, the quartz rich shales (Mancos) stayed strongly water wet in similar condition. The temperature effect was observed to be insignificant on the hydrophilicity of shale surface. Guiltinan et al.[224] studied the effect of $SC\text{-}CO_2$ on the wettability of shales with varying TOC and thermal maturity. They observed that the shale samples continued to be highly water-wet, despite the changes in the concentrations of organic matter and thermal maturities, because it was the mineralogy of the shale that dominated the wetting behavior. This indicated reservoirs, consisting of organic-rich caprocks, may be suitable for CO_2 sequestration. However, they concluded that the concentration of the organic matter must be below the percolation threshold (minimum porosity required to form connected pathways across a porous medium) for the organic matter to not have any influence on the wetting behavior.

7. CHALLENGES AND PERSPECTIVES

7.1. Changes in Porosity and Mineralogy Due to Shale-$SC\text{-}CO_2$ Interactions. One common observation from all of the above studies is the dissolution of primary porous structures and fractures, and reformation of newer porous structures and conduits in shales with increasing exposure to $SC\text{-}CO_2$. However, the changes in mineralogy and specific surface area can be observed to be variable for different researches. One of the limitations in the above studies is the variability of shales in terms of their organic composition, content, and thermal maturity levels, as in most of the studies, the shales can be observed to have minimal variation. For example, a molecular dynamics (MD)-based study of mineral-$SC\text{-}CO_2$ and OM-$SC\text{-}CO_2$ interaction has shown that the solid−liquid friction is lowest for OM-$SC\text{-}CO_2$, resulting in a larger slip length, which allows $SC\text{-}CO_2$ to penetrate even smaller micropores in shales very easily.[213] Therefore, studies focusing on shales with a range of TOC content and thermal maturity level can provide more insights toward the shale-$SC\text{-}CO_2$ interactions. Another critical factor that could possibly influence the interactions is the type of kerogen present within the shales. Laboratory investigations focused at the microscale have also revealed significant changes in elastic modulus of organic matter and minerals in shales after $SC\text{-}CO_2$ exposure.[226] The effect of $SC\text{-}CO_2$ could change, depending on the type of kerogen, and studies have shown that the change in micropore structure in shales for Type I kerogen is mostly due to adsorption-induced swelling. However, for Type II kerogen (TOC < 3%), the change is governed by pore framework reorganization due to dissolution of minerals.[203] Thus, because of their different chemistries and structure, different kerogens behave differently when studied in different environments,[227,228] and it is likely that, depending on the degree of aromatization, aliphatic content, and stability, the kerogens would respond uniquely when exposed to $SC\text{-}CO_2$.

7.2. Implications for CO_2 Sequestration. Several factors and interaction of processes must be considered and evaluated, especially when considering the advantages presented by $SC\text{-}CO_2$ for long-term sequestration of CO_2 in shale reservoirs. $SC\text{-}CO_2$, on one hand, aids in the creation of larger pores and pathways by dissolution of primary porous structures, minerals, organic matter, and creation of new conduits, which allows extraction of methane and distribution of CO_2 underground (favorable for CO_2 sequestration). On the other hand, changes in the structure of the shales caused by the creation of fractures and reduction of their strength (as seen in almost all studies) can pose major risks, because of potential leakage of CO_2 through these created pathways. In contrast to the observations of several researchers, that $SC\text{-}CO_2$ increases the permeability of shale reservoirs, Zhou et al.[229] observed CO_2-adsorption-induced shale matrix swelling. Similar observations on the swelling of a shale matrix due to $SC\text{-}CO_2$ have also been made by Memom et al.[230] Generally, the preferential adsorption of CO_2 in organic matter is accompanied by the swelling of organic matter due to multilayer adsorption in smaller pores exerting pressure on the pore walls, thereby resulting in their outward expansion.[231] Dissolution of organic matter and minerals, creation of fractures on one hand, and swelling of organic matrix due to CO_2 adsorption, thus indicates that a complex set of processes would be effective, especially when long-term sequestration of CO_2 is considered in deep reservoirs. Interaction of these processes would likely control the sealing capacity of shales, especially at field-scale. This point becomes especially critical when the duration of study in the laboratory, generally <30 days, is considered. A period of up to 40 years may be needed for a shale gas well, while the sequestered CO_2 needs to be stable for thousands of years.[34] Consequently, future studies should focus on the simulation and development of models for predicting the long-term storage potential of CO_2 in shale reservoirs.

Wettability of shales also presents certain critical aspects for them to be considered for CO_2 sequestration. Fatah et al.,[195] in their review of the CO_2/shale interactions on the shale properties, documented that the CO_2-wet shales can translate into a dramatic reduction of CO_2 storage capacity and sealing efficiency of the caprock. It is attributed to the increase in the contact angle between the CO_2 and shale, resulting in decreased capillary force and upward movement of CO_2 by the buoyancy forces, which ultimately increase the likelihood of capillary breakthrough. In contrast, when the shale caprock is strongly water wet, the upward movement of the sequestered CO_2 is restrained, because of the high capillary forces in the pore structures of the shale.[195,217] TOC and mineralogical composition play an important role in influencing the wettability alteration of shales. Shale−caprocks rich in clay minerals

https://doi.org/10.1021/acs.energyfuels.2c01894
Energy Fuels 2022, 36, 9882−9903

become CO_2-wet, whereas the quartz-rich shales remain strongly water-wet. Whether the wettability of TOC-rich shale be CO_2-wet or not is dependent on the percolation threshold. The theory of percolation threshold predicts that, in a medium of randomly distributed porosity, this threshold is met at ~12%.[232] However, if the organic matters present in the shales are in thin laminations, then the percolation threshold would be higher across lamination and lower in the direction perpendicular to it.[233−235] Therefore, it suggests that even if the percolation threshold is below or above 12%, the alteration in shale wettability would also be dependent on the direction of organic matter laminations, with respect to the direction of the upward-moving CO_2. Similarly, the presence and distribution of functional groups within shale surfaces have been observed to strongly influence the shale wettability behavior.[236] Future studies should evaluate these aspects. In a summary, the key parameters that affect the wettability of the shales are pressure, temperature, TOC, mineralogical composition, organic matter connectivity (percolation threshold), distribution, fluid properties, and surface chemistry.[195,217,237,238] However, further research is necessary in order to gain insights about the alteration of shale wettability when reservoir scale operations are considered.

8. CONCLUSION

The following conclusions are reached for this work:

- Hydraulic fracturing dominates the shale-gas extraction industry but its continued usage can negatively impact the environment and human health. CO_2 can be a better alternative to water at all stages of shale-gas exploration (i.e., drilling, fracturing, and injection), especially after its transition to a supercritical phase (also known as SC-CO_2) at 7.38 MPa and 31.1 °C.
- CO_2-based shale gas exploration presents dual benefits in the form of (a) being beneficial for enhanced production of shale gas, and (b) CO_2 geological sequestration, because of the preferential desorption of CH_4 by CO_2. In addition, SC-CO_2 is better at achieving a higher penetration rate during drilling, and it is capable of creating complex fracture networks with better stimulated reservoir volumes during fracturing.
- Some limitations of SC-CO_2, such as the poor cuttings and proppant carrying capacity, exist, predominantly due to its low viscosity. Chemical additives can be used to enhance the cuttings carrying ability, whereas the proppant carrying capacity can be increased using microproppants.
- The interaction of SC-CO_2 with the reservoir brings remarkable changes in the shale properties. The induced changes such as increase in surface area, fractal dimensions, formation of new porous structure, etc., are mostly favorable to the gas extraction and sequestration process. However, there still remains some level of ambiguity involved with such variations.
- The increase/decrease in the composition of some minerals, surface area, and fractal dimensions of the shale with increasing exposure to SC-CO_2 can be attributed to the variability of shales, in terms of their mineralogical composition, organic composition, and content, and thermal maturity levels. Future research works focusing on variety of shales with a range of TOC contents, kerogen types, and thermal maturity levels would provide more insights toward shale−SC-CO_2 interactions.
- The change in the mechanical properties of shales with increasing exposure to SC-CO_2 is due to the weakening of the microstructure of the shale primarily caused by mineral dissolution. The other factors include phase state of CO_2 and bedding angle. Again, because of the highly variable nature of shales, future studies shall focus more on the micromechanical variations of different mineral and organic matter phases within the rock using techniques such as nanoindentation, atomic force microscopy, etc.

AUTHOR INFORMATION

Corresponding Author

Vikram Vishal − *Department of Earth Sciences, Indian Institute of Technology Bombay, Mumbai 400076, India; National Centre of Excellence in Carbon Capture and Utilization and Interdisciplinary Programme in Climate Studies, Indian Institute of Technology Bombay, Mumbai 400076, India;* orcid.org/0000-0002-0896-7844; Phone: +91-22-2576-7254; Email: v.vishal@iitb.ac.in; Fax: +91-22-2576-7253; https://www.geos.iitb.ac.in/index.php/vv/

Authors

Bodhisatwa Hazra − *CSIR- Central Institute of Mining and Fuel Research, Dhanbad 826015, India; Academy of Scientific and Innovative Research (AcSIR), Ghaziabad 201002, India;* orcid.org/0000-0002-3462-7552

Chinmay Sethi − *CSIR- Central Institute of Mining and Fuel Research, Dhanbad 826015, India; Academy of Scientific and Innovative Research (AcSIR), Ghaziabad 201002, India*

Debanjan Chandra − *Department of Earth Sciences, Indian Institute of Technology Bombay, Mumbai 400076, India; Department of Geoscience and Engineering, Delft University of Technology, 2628 CN Delft, The Netherlands;* orcid.org/0000-0001-6093-7389

Complete contact information is available at: https://pubs.acs.org/10.1021/acs.energyfuels.2c01894

Notes

The authors declare no competing financial interest.

Biographies

Bodhisatwa Hazra is currently working as a Scientist at CSIR-Central Institute of Mining and Fuel Research, Dhanbad. He graduated with a doctoral degree from the Department of Applied Geology, Indian Institute of Technology (Indian School of Mines) Dhanbad. He specializes on hydrocarbon geosciences and is currently working on source rock geochemistry, petrophysics, CO_2 sequestration in shales, and chemistry and structure of dispersed organic matter.

Vikram Vishal is an Associate Professor in the Department of Earth Sciences, Indian Institute of Technology Bombay, Mumbai. He is an Associate Faculty in the Interdisciplinary Programme in Climate Studies at IIT Bombay. His research areas include reservoir geomechanics, unconventional petrophysics, and carbon sequestration. He holds a Bachelor's degree in Geology from University of Calcutta, a Master's degree in Applied Geology from IIT Bombay, and a Ph.D. degree from IIT Bombay and Monash University.

Chinmay Sethi is currently working as a doctoral student at CSIR-CIMFR. He is currently working on shale geomechanics, geochemistry, and petrophysics. Currently, he is focusing on developing the optical/

https://doi.org/10.1021/acs.energyfuels.2c01894
Energy Fuels 2022, 36, 9882−9903

electron correlative interface for mapping dispersed organic matter in shales. He received an M.Sc. degree in Applied Geology and Geoinformatics from Central University of Karnataka, India in 2019.

Debanjan Chandra is current working as a doctoral student in the Department of Earth Sciences, Indian Institute of Technology (IIT) Bombay. His Ph.D. work aims to understand the role of organic/inorganic composition of shales on the distribution and accessibility of pores, leading to shale gas recovery and carbon dioxide storage. He holds an M.Sc. degree in Geological Sciences and a B.Sc. degree in Geology, respectively, from IISER Kolkata, and Presidency University, Kolkata.

■ ACKNOWLEDGMENTS

The Director of CSIR-CIMFR is thankfully acknowledged for giving the necessary permission to publish this work. The Editor, and the anonymous reviewers, is thankfully acknowledged for their constructive comments.

■ REFERENCES

(1) Vishal, V.; Chandra, D.; Singh, U.; Verma, Y. Understanding Initial Opportunities and Key Challenges for CCUS Deployment in India at Scale. *Resour. Conserv. Recycl.* **2021**, *175*, 105829.
(2) Keith, D. W. Why Capture CO_2 from the Atmosphere? *Science* **2009**, *325* (5948), 1654−1655.
(3) Ding, K.; Zhong, D. L.; Lu, Y. Y.; Wang, J. Le. Enhanced Precombustion Capture of Carbon Dioxide by Gas Hydrate Formation in Water-In-Oil Emulsions. *Energy Fuels* **2015**, *29* (5), 2971−2978.
(4) Kerr, R. A. Natural Gas from Shale Bursts Onto the Scene. *Sci. Mag.* **2010**, *328* (June), 1624−1626.
(5) Jarvie, D. M.; Hill, R. J.; Ruble, T. E.; Pollastro, R. M. Unconventional Shale-Gas Systems: The Mississippian Barnett Shale of North-Central Texas as One Model for Thermogenic Shale-Gas Assessment. *Am. Assoc. Pet. Geol. Bull.* **2007**, *91* (4), 475−499.
(6) Wood, D. A.; Hazra, B. Characterization of organic-rich shales for petroleum exploration & exploitation: A review-Part 1: Bulk properties, multi-scale geometry and gas adsorption. *J. Earth Sci.* **2017**, *28* (5), 739−757.
(7) Vishal, V.; Chandra, D.; Bahadur, J.; Sen, D.; Hazra, B.; Mahanta, B.; Mani, D. Interpreting Pore Dimensions in Gas Shales Using a Combination of SEM Imaging, Small-Angle Neutron Scattering, and Low-Pressure Gas Adsorption. *Energy Fuels* **2019**, *33* (6), 4835−4848.
(8) Boykoff, M.; Pearman, O. Now or never: How media coverage of the IPCC special report on 1.5 C shaped climate-action deadlines. *One Earth* **2019**, *1* (3), 285−288.
(9) Rogelj, J.; Schaeffer, M.; Meinshausen, M.; Knutti, R.; Alcamo, J.; Riahi, K.; Hare, W. Zero Emission Targets as Long-Term Global Goals for Climate Protection. *Environ. Res. Lett.* **2015**, *10* (10), 105007.
(10) Rogelj, J.; Popp, A.; Calvin, K. V.; Luderer, G.; Emmerling, J.; Gernaat, D.; Fujimori, S.; Strefler, J.; Hasegawa, T.; Marangoni, G.; Krey, V.; Kriegler, E.; Riahi, K.; Van Vuuren, D. P.; Doelman, J.; Drouet, L.; Edmonds, J.; Fricko, O.; Harmsen, M.; Havlík, P.; Humpenöder, F.; Stehfest, E.; Tavoni, M. Scenarios towards Limiting Global Mean Temperature Increase below 1.5° C. *Nat. Clim. Chang.* **2018**, *8* (4), 325−332.
(11) Vishal, V.; Verma, Y.; Chandra, D.; Ashok, D. A Systematic Capacity Assessment and Classification of Geologic CO_2 Storage Systems in India. *Int. J. Greenh. Gas Control* **2021**, *111*, 103458.
(12) Xie, W.; Chen, S.; Wang, M.; Yu, Z.; Wang, H. Progress and Prospects of Supercritical CO_2 Application in the Exploitation of Shale Gas Reservoirs. *Energy Fuels* **2021**, *35* (22), 18370−18384.
(13) Luderer, G.; Vrontisi, Z.; Bertram, C.; Edelenbosch, O. Y.; Pietzcker, R. C.; Rogelj, J.; De Boer, H. S.; Drouet, L.; Emmerling, J.; Fricko, O.; Fujimori, S.; Havlík, P.; Iyer, G.; Keramidas, K.; Kitous, A.; Pehl, M.; Krey, V.; Riahi, K.; Saveyn, B.; Tavoni, M.; Van Vuuren, D. P.; Kriegler, E. Residual Fossil CO_2 Emissions in 1.5−2° C Pathways. *Nat. Clim. Chang* **2018**, *8* (7), 626−633.
(14) IPCC. Underground geological storage. In *IPCC Special Report on Carbon Dioxide Capture and Storage*, prepared by Working Group III of the Intergovernmental Panel on Climate Change; Metz, B., Davidson, O., de Coninck, H. C., Loos, M., Meyer, L. A., Eds.; Cambridge University Press: Cambridge, U.K., and New York, USA, 2005; pp 195−276.
(15) Oh, T. H. Carbon Capture and Storage Potential in Coal-Fired Plant in Malaysia - A Review. *Renew. Sustain. Energy Rev.* **2010**, *14* (9), 2697.
(16) Cuéllar-Franca, R. M.; Azapagic, A. Carbon Capture, Storage and Utilisation Technologies: A Critical Analysis and Comparison of Their Life Cycle Environmental Impacts. *J. CO_2 Util.* **2015**, *9*, 82−102.
(17) Vishal, V. Saturation Time Dependency of Liquid and Supercritical CO_2 permeability of Bituminous Coals: Implications for Carbon Storage. *Fuel* **2017**, *192*, 201−207.
(18) Metz, B.; Davidson, O.; De Coninck, H. C.; Loos, M.; Meyer, L. *IPCC Special Report on Carbon Dioxide Capture and Storage*; Cambridge University Press: Cambridge, U.K., 2005.
(19) Bachu, S. CO_2 Storage in Geological Media: Role, Means, Status and Barriers to Deployment. *Prog. Energy Combust. Sci.* **2008**, *34* (2), 254−273.
(20) Goodman, A.; Kutchko, B.; Sanguinito, S.; Natesakhawat, S.; Cvetic, P.; Haljasmaa, I.; Spaulding, R.; Crandall, D.; Moore, J.; Burrows, L. C. Reactivity of CO_2 with Utica, Marcellus, Barnett, and Eagle Ford Shales and impact on permeability. *Energy Fuels* **2021**, *35* (19), 15894−15917.
(21) Orr, F. M., Jr; Taber, J. J. Use of carbon dioxide in enhanced oil recovery. *Science* **1984**, *224* (4649), 563−569.
(22) Sharma, S.; Agrawal, V.; McGrath, S.; Hakala, J. A.; Lopano, C.; Goodman, A. Geochemical Controls on CO_2 interactions with Deep Subsurface Shales: Implications for Geologic Carbon Sequestration. *Environ. Sci. Process. Impacts* **2021**, *23* (9), 1278−1300.
(23) Montgomery, S.; Jarvie, D.; Bowker, K.; Pollastro, R. Mississippian Barnett shale, Fort Worth basin, north-central Texas: gas-shale play with multi-trillion cubic foot potential. *Am. Assoc. Pet. Geol. Bull.* **2005**, *89*, 155e175.
(24) Ross, D. J. K.; Marc Bustin, R. The Importance of Shale Composition and Pore Structure upon Gas Storage Potential of Shale Gas Reservoirs. *Mar. Pet. Geol.* **2009**, *26* (6), 916−927.
(25) Nuttal, B. C.; Eble, C.; Bustin, R. M.; Drahovzal, J. A. Analysis of Devonian Black Shales in Kentucky for Potential Carbon Dioxide Sequestration and Enhanced Natural Gas Production. *Greenh. Gas Control Technol.* **2005**, *II*, 2225−2228.
(26) Tao, Z.; Clarens, A. Estimating the Carbon Sequestration Capacity of Shale Formations Using Methane Production Rates. *Environ. Sci. Technol.* **2013**, *47* (19), 11318−11325.
(27) Godec, M.; Koperna, G.; Petrusak, R.; Oudinot, A. Potential for Enhanced Gas Recovery and CO_2 Storage in the Marcellus Shale in the Eastern United States. *Int. J. Coal Geol.* **2013**, *118*, 95−104.
(28) Heller, R.; Zoback, M. Adsorption of Methane and Carbon Dioxide on Gas Shale and Pure Mineral Samples. *J. Unconv. Oil Gas Resour.* **2014**, *8* (C), 14−24.
(29) Ma, L.; Fauchille, A. L.; Ansari, H.; Chandler, M.; Ashby, P.; Taylor, K.; Pini, R.; Lee, P. D. Linking Multi-Scale 3D Microstructure to Potential Enhanced Natural Gas Recovery and Subsurface CO2storage for Bowland Shale. *UK. Energy Environ. Sci.* **2021**, *14* (8), 4481−4498.
(30) Chalmers, G. R. L.; Bustin, R. M. Lower Cretaceous Gas Shales in Northeastern British Columbia, Part I: Geological Controls on Methane Sorption Capacity. *Bull. Can. Pet. Geol.* **2008**, *56* (1), 1−21.
(31) Loucks, R. G.; Reed, R. M.; Ruppel, S. C.; Jarvie, D. M. Morphology, Genesis, and Distribution of Nanometer-Scale Pores in Siliceous Mudstones of the Mississippian Barnett Shale. *J. Sediment. Res.* **2009**, *79* (12), 848−861.
(32) Hazra, B.; Wood, D. A.; Vishal, V.; Varma, A. K.; Sakha, D.; Singh, A. K. Porosity Controls and Fractal Disposition of Organic-Rich Permian Shales Using Low-Pressure Adsorption Techniques. *Fuel* **2018**, *220*, 837−848.

https://doi.org/10.1021/acs.energyfuels.2c01894
Energy Fuels 2022, 36, 9882−9903

(33) Hazra, B.; Vishal, V.; Singh, D. P. Applicability of Low-Pressure CO_2 and N2Adsorption in Determining Pore Attributes of Organic-Rich Shales and Coals. *Energy Fuels* **2021**, *35* (1), 456−464.
(34) Lyu, Q.; Tan, J.; Li, L.; Ju, Y.; Busch, A.; Wood, D. A.; Ranjith, P. G.; Middleton, R.; Shu, B.; Hu, C.; Wang, Z.; Hu, R. The Role of Supercritical Carbon Dioxide for Recovery of Shale Gas and Sequestration in Gas Shale Reservoirs. *Energy Environ. Sci.* **2021**, *14* (8), 4203−4227.
(35) Pan, Y.; Hui, D.; Luo, P.; Zhang, Y.; Sun, L.; Wang, K. Experimental investigation of the geochemical interactions between supercritical CO_2 and shale: implications for CO_2 storage in gas-bearing shale formations. *Energy Fuels* **2018**, *32* (2), 1963−1978.
(36) Yang, J.; Lian, H.; Liang, W.; Nguyen, V. P.; Chen, Y. Experimental Investigation of the Effects of Supercritical Carbon Dioxide on Fracture Toughness of Bituminous Coals. *Int. J. Rock Mech. Min. Sci.* **2018**, *107*, 233−242.
(37) Ishida, T.; Aoyagi, K.; Niwa, T.; Chen, Y.; Murata, S.; Chen, Q.; Nakayama, Y. Acoustic Emission Monitoring of Hydraulic Fracturing Laboratory Experiment with Supercritical and Liquid CO_2. *Geophys. Res. Lett.* **2012**, *39* (16), 1−6.
(38) Zhou, J.; Liu, M.; Xian, X.; Jiang, Y.; Liu, Q.; Wang, X. Measurements and Modelling of CH_4 and CO_2 Adsorption Behaviors on Shales: Implication for CO_2 Enhanced Shale Gas Recovery. *Fuel* **2019**, *251*, 293−306.
(39) Zhang, H.; Diao, R.; Chan, H. H.; Mostofi, M.; Evans, B. Molecular Simulation of the Adsorption-Induced Deformation during CO_2 Sequestration in Shale and Coal Carbon Slit Pores. *Fuel* **2020**, *272*, No. 117693.
(40) Middleton, R. S.; Carey, J. W.; Currier, R. P.; Hyman, J. D.; Kang, Q.; Karra, S.; Jiménez-Martínez, J.; Porter, M. L.; Viswanathan, H. S. Shale Gas and Non-Aqueous Fracturing Fluids: Opportunities and Challenges for Supercritical CO_2. *Appl. Energy* **2015**, *147*, 500−509.
(41) Zhang, K.; Cheng, Y.; Jin, K.; Guo, H.; Liu, Q.; Dong, J.; Li, W. Effects of supercritical CO_2 fluids on pore morphology of coal: implications for CO_2 geological sequestration. *Energy Fuels* **2017**, *31* (5), 4731−4741.
(42) Kohl, T.; Mégel, T. Predictive Modeling of Reservoir Response to Hydraulic Stimulations at the European EGS Site Soultz-Sous-Forêts. *Int. J. Rock Mech. Min. Sci.* **2007**, *44* (8), 1118−1131.
(43) Rahm, D. Regulating Hydraulic Fracturing in Shale Gas Plays: The Case of Texas. *Energy Policy* **2011**, *39* (5), 2974−2981.
(44) Tan, P.; Jin, Y.; Han, K.; Hou, B.; Chen, M.; Guo, X.; Gao, J. Analysis of Hydraulic Fracture Initiation and Vertical Propagation Behavior in Laminated Shale Formation. *Fuel* **2017**, *206*, 482−493.
(45) Wanniarachchi, W. A. M.; Ranjith, P. G.; Perera, M. S. A.; Rathnaweera, T. D.; Zhang, D. C.; Zhang, C. Investigation of Effects of Fracturing Fluid on Hydraulic Fracturing and Fracture Permeability of Reservoir Rocks: An Experimental Study Using Water and Foam Fracturing. *Eng. Fract. Mech.* **2018**, *194*, 117−135.
(46) Vengosh, A.; Jackson, R. B.; Warner, N.; Darrah, T. H.; Kondash, A. A Critical Review of the Risks to Water Resources from Unconventional Shale Gas Development and Hydraulic Fracturing in the United States. *Environ. Sci. Technol.* **2014**, *48* (15), 8334−8348.
(47) Kargbo, D. M.; Wilhelm, R. G.; Campbell, D. J. Natural Gas Plays in the Marcellus Shale: Challenges and Potential Opportunities. *Environ. Sci. Technol.* **2010**, *44* (15), 5679−5684.
(48) Howarth, R. W.; Ingraffea, A.; Engelder, T. Natural Gas: Should Fracking Stop? *Nature* **2011**, *477* (7364), 271−275.
(49) Rozell, D. J.; Reaven, S. J. Water Pollution Risk Associated with Natural Gas Extraction from the Marcellus Shale. *Risk Anal.* **2012**, *32* (8), 1382−1393.
(50) Vidic, R. D.; Brantley, S. L.; Vandenbossche, J. M.; Yoxtheimer, D.; Abad, J. D. Impact of Shale Gas Development on Regional Water Quality. *Science.* **2013**, *340* (6134), 1235009.
(51) Vengosh, A.; Warner, N.; Jackson, R.; Darrah, T. The Effects of Shale Gas Exploration and Hydraulic Fracturing on the Quality of Water Resources in the United States. *Procedia Earth Planet. Sci.* **2013**, *7*, 863−866.
(52) Ferrar, K. J.; Kriesky, J.; Christen, C. L.; Marshall, L. P.; Malone, S. L.; Sharma, R. K.; Michanowicz, D. R.; Goldstein, B. D. Assessment and Longitudinal Analysis of Health Impacts and Stressors Perceived to Result from Unconventional Shale Gas Development in the Marcellus Shale Region. *Int. J. Occup. Environ. Health* **2013**, *19* (2), 104−112.
(53) Pacsi, A. P.; Alhajeri, N. S.; Zavala-Araiza, D.; Webster, M. D.; Allen, D. T. Regional Air Quality Impacts of Increased Natural Gas Production and Use in Texas. *Environ. Sci. Technol.* **2013**, *47* (7), 3521−3527.
(54) Olmstead, S. M.; Muehlenbachs, L. A.; Shih, J. S.; Chu, Z.; Krupnick, A. J. Shale Gas Development Impacts on Surface Water Quality in Pennsylvania. *Proc. Natl. Acad. Sci. U. S. A.* **2013**, *110* (13), 4962−4967.
(55) Warner, N. R.; Kresse, T. M.; Hays, P. D.; Down, A.; Karr, J. D.; Jackson, R. B.; Vengosh, A. Geochemical and Isotopic Variations in Shallow Groundwater in Areas of the Fayetteville Shale Development, North-Central Arkansas. *Appl. Geochem.* **2013**, *35*, 207−220.
(56) Warner, N. R.; Christie, C. A.; Jackson, R. B.; Vengosh, A. Impacts of Shale Gas Wastewater Disposal on Water Quality in Western Pennsylvania. *Environ. Sci. Technol.* **2013**, *47* (20), 11849−11857.
(57) Scanlon, B. R.; Reedy, R. C.; Nicot, J. P. Comparison of Water Use for Hydraulic Fracturing for Unconventional Oil and Gas versus Conventional Oil. *Environ. Sci. Technol.* **2014**, *48* (20), 12386−12393.
(58) Engelder, T. Capillary Tension and Imbibition Sequester Frack Fluid in Marcellus Gas Shale. *Proc. Natl. Acad. Sci. U. S. A.* **2012**, *109* (52), 3625.
(59) Warner, N. R.; Jackson, R. B.; Darrah, T. H.; Osborn, S. G.; Down, A.; Zhao, K.; White, A.; Vengosh, A. Geochemical Evidence for Possible Natural Migration of Marcellus Formation Brine to Shallow Aquifers in Pennsylvania. *Proc. Natl. Acad. Sci. U. S. A.* **2012**, *109* (30), 11961−11966.
(60) Elsworth, D.; Spiers, C. J.; Niemeijer, A. R. Understanding Induced Seismicity. *Science (80-.)* **2016**, *354* (6318), 1380−1381.
(61) Currie, J.; Greenstone, M.; Meckel, K. Hydraulic Fracturing and Infant Health: New Evidence from Pennsylvania. *Sci. Adv.* **2017**, *3* (12), e1603021.
(62) Schimmel, M.; Liu, W.; Worrell, E. Facilitating Sustainable Geo-Resources Exploitation: A Review of Environmental and Geological Risks of Fluid Injection into Hydrocarbon Reservoirs. *Earth-Science Rev.* **2019**, *194*, 455−471.
(63) Lyu, Q.; PG, R.; Long, X.; Kang, Y.; Huang, M. Effects of Coring Directions on the Mechanical Properties of Chinese Shale. *Arab. J. Geosci.* **2015**, *8* (12), 10289−10299.
(64) Lyu, Q.; Long, X.; Ranjith, P. G.; Tan, J.; Kang, Y.; Wang, Z. Experimental Investigation on the Mechanical Properties of a Low-Clay Shale with Different Adsorption Times in Sub-/Super-Critical CO_2. *Energy* **2018**, *147*, 1288−1298.
(65) Shen, Y.; Ge, H.; Meng, M.; Jiang, Z.; Yang, X. Effect of Water Imbibition on Shale Permeability and Its Influence on Gas Production. *Energy Fuels* **2017**, *31* (5), 4973−4980.
(66) Liang, T.; Zhou, F.; Lu, J.; DiCarlo, D.; Nguyen, Q. Evaluation of Wettability Alteration and IFT Reduction on Mitigating Water Blocking for Low-Permeability Oil-Wet Rocks after Hydraulic Fracturing. *Fuel* **2017**, *209* (July), 650−660.
(67) Zolfaghari, A.; Dehghanpour, H.; Holyk, J. Water Sorption Behaviour of Gas Shales: I. *Role of Clays. Int. J. Coal Geol.* **2017**, *179*, 130−138.
(68) Middleton, R.; Viswanathan, H.; Currier, R.; Gupta, R. CO_2 as a Fracturing Fluid: Potential for Commercial-Scale Shale Gas Production and CO_2 Sequestration. *Energy Procedia* **2014**, *63*, 7780−7784.
(69) Zhang, X.; Wang, J. G.; Gao, F.; Ju, Y. Impact of Water, Nitrogen and CO_2 Fracturing Fluids on Fracturing Initiation Pressure and Flow Pattern in Anisotropic Shale Reservoirs. *J. Nat. Gas Sci. Eng.* **2017**, *45*, 291−306.
(70) Zhao, Z.; Li, X.; He, J.; Mao, T.; Zheng, B.; Li, G. A Laboratory Investigation of Fracture Propagation Induced by Supercritical Carbon Dioxide Fracturing in Continental Shale with Interbeds. *J. Pet. Sci. Eng.* **2018**, *166*, 739−746.

https://doi.org/10.1021/acs.energyfuels.2c01894
Energy Fuels 2022, 36, 9882−9903

(71) Yang, J.; Lian, H.; Li, L. Fracturing in Coals with Different Fluids: An Experimental Comparison between Water, Liquid CO_2, and Supercritical CO_2. *Sci. Rep.* **2020**, *10* (1), 1−15.
(72) Kolle, J. J. Coiled-tubing drilling with supercritical carbon dioxide. Presented at *SPE/Petroleum Society of CIM International Conference on Horizontal Well Technology*. Nov. 6−8, 2000, Calgary, Alberta, Canada; SPE Paper No. 65534, DOI: 10.2523/65534-ms.
(73) Burrows, L. C.; Haeri, F.; Cvetic, P.; Sanguinito, S.; Shi, F.; Tapriyal, D.; Goodman, A.; Enick, R. M. A Literature Review of CO_2, Natural Gas, and Water-Based Fluids for Enhanced Oil Recovery in Unconventional Reservoirs. *Energy Fuels* **2020**, *34* (5), 5331−5380.
(74) Gupta, A. P.; Gupta, A.; Langlinais, J. Feasibility of supercritical carbon dioxide as a drilling fluid for deep underbalanced drilling operation. Presented at *Annual Technical Conference and Exhibition*, Oct. 9−12, Dallas, TX, 2005, SPE Paper No. 96992.
(75) Shahbazi, K.; Mehta, S. A.; Moore, R. G.; Ursenbach, M. G.; Fraassen, K. C. V. Investigation of Explosion Occurrence in Underbalanced Drilling. *SPE Prod. Oper. Symp. Proc.* **2007**, 427−434.
(76) Herzhaft, B.; Toure, A.; Bruni, F.; Saintpere, S. Aqueous Foams for Underbalanced Drilling: The Question of Solids. *SPE Reserv. Eng.* **2000**, *A*, 101−113.
(77) Maranuk, C.; Rodriguez, A.; Trapasso, J.; Watson, J. Unique System for Underbalanced Drilling Using Air in the Marcellus Shale. *SPE East. Reg. Meet.* **2014**, *2014*, 239−249.
(78) Qutob, H.; Byrne, M. Formation Damage in Tight Gas Reservoirs. *SPE - Eur. Form. Damage Conf. Proceedings, EFDC* **2015**, *2015*, 449−466.
(79) Tian, S.; He, Z.; Li, G.; Wang, H.; Shen, Z.; Liu, Q. Influences of Ambient Pressure and Nozzle-to-Target Distance on SC-CO_2 Jet Impingement and Perforation. *J. Nat. Gas Sci. Eng.* **2016**, *29*, 232−242.
(80) Wang, H.; Shen, Z.; Li, G. The Development and Prospect of Supercritical Carbon Dioxide Drilling. *Pet. Sci. Technol.* **2012**, *30* (16), 1670−1676.
(81) Shen, Z.; Wang, H.; Li, G. Feasibility Analysis of Coiled Tubing Drilling with Supercritical Carbon Dioxide. *Pet. Explor. Dev.* **2010**, *37* (6), 743−747.
(82) Bahrami, H.; Rezaee, R.; Ostojic, J.; Nazhat, D.; Clennell, B. Evaluation of Damage Mechanisms and Skin Factor in Tight Gas Reservoirs. *Soc. Pet. Eng. - 9th Eur. Form. Damage Conf.* **2011**, *1*, 47−57.
(83) Civan, F. Multi-Phase Mud Filtrate Invasion and Wellbore Filter Cake Formation Model. In *Proceedings of International Petroleum Conference and Exhibition of Mexico*, 1994; Society of Petroleum Engineers, pp 399−412, DOI: 10.2523/28709-ms.
(84) Windarto; Gunawan, A. Y.; Sukarno, P.; Soewono, E. Modelling of Formation Damage Due to Mud Filtrate Invasion in a Radial Flow System. *J. Pet. Sci. Eng.* **2012**, *100*, 99−105.
(85) Liu, Y.; Guo, X.; Wei, J.; Zhang, H. Application of Supercritical Carbon Dioxide Jet: A Parametric Study Using Numerical Simulation Model. *J. Pet. Sci. Eng.* **2021**, *201*, 108422.
(86) Shen, Z.; Wang, H.; Li, G. Numerical Simulation of the Cutting-Carrying Ability of Supercritical Carbon Dioxide Drilling at Horizontal Section. *Pet. Explor. Dev.* **2011**, *38* (2), 233−236.
(87) Qin, C.; Jiang, Y.; Luo, Y.; Xian, X.; Liu, H.; Li, Y. Effect of Supercritical Carbon Dioxide Treatment Time, Pressure, and Temperature on Shale Water Wettability. *Energy Fuels* **2017**, *31* (1), 493−503.
(88) Raventós, M.; Duarte, S.; Alarcón, R. Application and Possibilities of Supercritical CO_2 Extraction in Food Processing Industry: An Overview. *Food Sci. Technol. Int.* **2002**, *8* (5), 269−284.
(89) Haizhu, W.; Zhonghou, S.; Gensheng, L. Influences of Formation Water Invasion on the Wellbore Temperature and Pressure in Supercritical CO_2 Drilling. *Pet. Explor. Dev.* **2011**, *38* (3), 362−368.
(90) Long, X.; Liu, Q.; Ruan, X.; Kang, Y.; Lyu, Q. *Numerical Investigation of the Flow of Supercritical Carbon Dioxide Injected into the Bottom Hole during Drilling with Special Emphasis on the Real Gas Effects*; Elsevier, 2016; Vol. 34. DOI: 10.1016/j.jngse.2016.08.003.
(91) Huang, M.; Kang, Y.; Wang, X.; Hu, Y.; Cai, C.; Liu, Y.; Chen, H. Experimental Investigation on the Rock Erosion Characteristics of a Self-Excited Oscillation Pulsed Supercritical CO_2 Jet. *Appl. Therm. Eng.* **2018**, *139* (April), 445−455.
(92) Ansaloni, L.; Alcock, B.; Peters, T. A. Effects of CO_2 on Polymeric Materials in the CO_2 Transport Chain: A Review. *Int. J. Greenh. Gas Control* **2020**, *94*, 102930.
(93) Hou, L.; Sun, B.; Geng, X.; Jiang, T.; Wang, Z. Study of the Slippage of Particle/Supercritical CO_2 Two-Phase Flow. *J. Supercrit. Fluids* **2017**, *120*, 173−180.
(94) Zhou, Y.; Ni, H.; Shen, Z.; Zhao, M. Study on Particle Settling in Supercritical Carbon Dioxide Drilling and Fracturing. *J. Pet. Sci. Eng.* **2020**, *190*, 107061.
(95) Yin, H.; Zhou, J.; Jiang, Y.; Xian, X.; Liu, Q. Physical and Structural Changes in Shale Associated with Supercritical CO_2 Exposure. *Fuel* **2016**, *184*, 289−303.
(96) Zhou, D.; Zhang, G.; Zhao, P.; Wang, Y.; Xu, S. Effects of Post-Instability Induced by Supercritical CO_2 Phase Change on Fracture Dynamic Propagation. *J. Pet. Sci. Eng.* **2018**, *162*, 358−366.
(97) Fatah, A.; Ben Mahmud, H.; Bennour, Z.; Hossain, M.; Gholami, R. Effect of Supercritical CO_2 Treatment on Physical Properties and Functional Groups of Shales. *Fuel* **2021**, *303* (May), No. 121310.
(98) Chen, H.; Hu, Y.; Kang, Y.; Cai, C.; Liu, J.; Liu, Y. Fracture Initiation and Propagation under Different Perforation Orientation Angles in Supercritical CO_2 Fracturing. *J. Pet. Sci. Eng.* **2019**, *183*, 106403.
(99) Yuan, Q.; Zhu, X.; Lin, K.; Zhao, Y. P. Molecular Dynamics Simulations of the Enhanced Recovery of Confined Methane with Carbon Dioxide. *Phys. Chem. Chem. Phys.* **2015**, *17* (47), 31887−31893.
(100) Qin, C.; Jiang, Y.; Zuo, S.; Chen, S.; Xiao, S.; Liu, Z. Investigation of Adsorption Kinetics of CH_4 and CO_2 on Shale Exposure to Supercritical CO_2. *Energy* **2021**, *236*, No. 121410.
(101) Liu, Q. Y.; Tao, L.; Zhu, H. Y.; Lei, Z. D.; Jiang, S.; McLennan, J. D. Macroscale Mechanical and Microscale Structural Changes in Chinese Wufeng Shale with Supercritical Carbon Dioxide Fracturing. *SPE J.* **2018**, *23* (3), 691−703.
(102) Liu, D.; Yang, S.; Li, Y.; Agarwal, R. A Review of Coupled Geo-Chemo-Mechanical Impacts of CO 2-Shale Interaction on Enhanced Shale Gas Recovery. *Sustainable Agriculture Reviews* **2019**, *37*, 107−126.
(103) Zhang, X.; Lu, Y.; Tang, J.; Zhou, Z.; Liao, Y. Experimental Study on Fracture Initiation and Propagation in Shale Using Supercritical Carbon Dioxide Fracturing. *Fuel* **2017**, *190*, 370−378.
(104) Wang, L.; Yao, B.; Xie, H.; Winterfeld, P. H.; Kneafsey, T. J.; Yin, X.; Wu, Y. S. CO_2 Injection-Induced Fracturing in Naturally Fractured Shale Rocks. *Energy* **2017**, *139*, 1094−1110.
(105) Wang, J.; Elsworth, D.; Wu, Y.; Liu, J.; Zhu, W.; Liu, Y. The Influence of Fracturing Fluids on Fracturing Processes: A Comparison Between Water, Oil and SC-CO_2. *Rock Mech. Rock Eng.* **2018**, *51* (1), 299−313.
(106) Ha, S. J.; Choo, J.; Yun, T. S. Liquid CO_2 Fracturing: Effect of Fluid Permeation on the Breakdown Pressure and Cracking Behavior. *Rock Mech. Rock Eng.* **2018**, *51* (11), 3407−3420.
(107) Ishida, T.; Chen, Y.; Bennour, Z.; Yamashita, H.; Inui, S.; Nagaya, Y.; Naoi, M.; Chen, Q.; Nakayama, Y.; Nagano, Y. Features of CO_2 Fracturing Deduced from Acoustic Emission and Microscopy in Laboratory Experiments. *J. Geophys. Res. Solid Earth* **2016**, *121* (11), 8080−8098.
(108) Bennour, Z.; Watanabe, S.; Chen, Y.; Ishida, T.; Akai, T. Evaluation of Stimulated Reservoir Volume in Laboratory Hydraulic Fracturing with Oil, Water and Liquid Carbon Dioxide under Microscopy Using the Fluorescence Method. *Geomech. Geophys. Geo-Energy Geo-Resources* **2018**, *4* (1), 39−50.
(109) Wang, J.; Elsworth, D. Fracture Penetration and Proppant Transport in Gas- and Foam-Fracturing. *J. Nat. Gas Sci. Eng.* **2020**, *77*, 103269.
(110) Zhou, Y.; Ni, H.; Shen, Z.; Zhao, M. Study on Particle Settling in Supercritical Carbon Dioxide Drilling and Fracturing. *J. Pet. Sci. Eng.* **2020**, *190*, 107061.
(111) Zhang, C. P.; Liu, S.; Ma, Z. Y.; Ranjith, P. G. Combined Micro-Proppant and Supercritical Carbon Dioxide (SC-CO_2) Fracturing in Shale Gas Reservoirs: A Review. *Fuel* **2021**, *305*, 121431.

(112) Ahn, C. H.; Chang, O. C.; Dilmore, R.; Wang, J. Y. A Hydraulic Fracture Network Propagation Model in Shale Gas Reservoirs: Parametric Studies to Enhance the Effectiveness of Stimulation. *Soc. Pet. Eng. - SPE/AAPG/SEG Unconv. Resour. Technol. Conf.* **2014**, 1−16.
(113) Aslannezhad, M.; Kalantariasl, A.; You, Z.; Iglauer, S.; Keshavarz, A. Micro-Proppant Placement in Hydraulic and Natural Fracture Stimulation in Unconventional Reservoirs: A Review. *Energy Reports* **2021**, *7*, 8997−9022.
(114) Fallahzadeh, S. H.; Shadizadeh, S. R.; Pourafshary, P. Dealing with the Challenges of Hydraulic Fracture Initiation in Deviated-Cased Perforated Boreholes. *Soc. Pet. Eng. - Trinidad Tobago Energy Resour. Conf. 2010, SPE TT 2010* **2010**, *1*, 475−489.
(115) Xie, J.; Cheng, W.; Wang, R.; Jiang, G.; Sun, D.; Sun, J. Experiments and Analysis on the Influence of Perforation Mode on Hydraulic Fracture Geometry in Shale Formation. *J. Pet. Sci. Eng.* **2018**, *168* (April), 133−147.
(116) Chen, M.; Jiang, H.; Zhang, G. Q.; Jin, Y. The Experimental Investigation of Fracture Propagation Behavior and Fracture Geometry in Hydraulic Fracturing through Oriented Perforations. *Pet. Sci. Technol.* **2010**, *28* (13), 1297−1306.
(117) Lei, X.; Zhang, S.; Xu, G.; Zou, Y. Impact of Perforation on Hydraulic Fracture Initiation and Extension in Tight Natural Gas Reservoirs. *Energy Technol.* **2015**, *3* (6), 618−624.
(118) Wang, H.; Li, G.; He, Z.; Tian, S.; Wang, M.; Yang, B.; Lu, Q.; Weng, L. Experimental Investigation on Abrasive Supercritical CO_2 Jet Perforation. *J. CO_2 Util.* **2018**, *28*, 59−65.
(119) Li, X.; He, Y.; Huo, M.; Yang, Z.; Wang, H.; Song, R. Model for Calculating the Temperature and Pressure within the Fracture during Supercritical Carbon Dioxide Fracturing. *Int. J. Hydrogen Energy* **2020**, *45* (15), 8369−8384.
(120) Zhou, D.; Zhang, G.; Prasad, M.; Wang, P. The Effects of Temperature on Supercritical CO_2 Induced Fracture: An Experimental Study. *Fuel* **2019**, *247*, 126−134.
(121) Gong, L.; Chen, S.; Zuo, J.; Bai, B.; Bai, Z. Phase Prediction of Supercritical Carbon Dioxide and Its Application in Fracturing Oil Wellbores. *J. Therm. Sci.* **2019**, *28* (3), 484−493.
(122) Zhang, Y.; He, J.; Li, X.; Lin, C. Experimental Study on the Supercritical CO_2 Fracturing of Shale Considering Anisotropic Effects. *J. Pet. Sci. Eng.* **2019**, *173*, 932−940.
(123) Jia, Y.; Song, C.; Wang, J.; Gan, Q. The Breakdown Process of Low-Permeable Shale and High-Permeable Sandstone Rocks Due to Non-Aqueous Fracturing: The Role of Fluid Infiltration. *J. Nat. Gas Sci. Eng.* **2021**, *89*, 103873.
(124) Vilarrasa, V.; Carrera, J.; Olivella, S.; Rutqvist, J.; Laloui, L. Induced Seismicity in Geologic Carbon Storage. *Solid Earth* **2019**, *10* (3), 871−892.
(125) Heller, R.; Zoback, M. Adsorption of Methane and Carbon Dioxide on Gas Shale and Pure Mineral Samples. *J. Unconv. Oil Gas Resour.* **2014**, *8* (C), 14−24.
(126) Zhou, J.; Xie, S.; Jiang, Y.; Xian, X.; Liu, Q.; Lu, Z.; Lyu, Q. Influence of supercritical CO_2 exposure on CH_4 and CO_2 adsorption behaviors of shale: implications for CO_2 sequestration. *Energy Fuels* **2018**, *32* (5), 6073−6089.
(127) Godec, M.; Koperna, G.; Petrusak, R.; Oudinot, A. Enhanced Gas Recovery and CO_2 Storage in Gas Shales: A Summary Review of Its Status and Potential. *Energy Procedia* **2014**, *63*, 5849−5857.
(128) Huang, L.; Ning, Z.; Wang, Q.; Zhang, W.; Cheng, Z.; Wu, X.; Qin, H. Effect of Organic Type and Moisture on CO_2/CH_4 Competitive Adsorption in Kerogen with Implications for CO_2 Sequestration and Enhanced CH_4 Recovery. *Appl. Energy* **2018**, *210*, 28−43.
(129) Wang, T.; Tian, S.; Li, G.; Sheng, M.; Ren, W.; Liu, Q.; Zhang, S. Molecular Simulation of CO_2/CH_4 Competitive Adsorption on Shale Kerogen for CO_2 Sequestration and Enhanced Gas Recovery. *J. Phys. Chem. C* **2018**, *122* (30), 17009−17018.
(130) Weniger, P.; Kalkreuth, W.; Busch, A.; Krooss, B. M. High-Pressure Methane and Carbon Dioxide Sorption on Coal and Shale Samples from the Paraná Basin, Brazil. *Int. J. Coal Geol.* **2010**, *84* (3−4), 190−205.
(131) Chareonsuppanimit, P.; Mohammad, S. A.; Robinson, R. L.; Gasem, K. A. M. High-Pressure Adsorption of Gases on Shales: Measurements and Modeling. *Int. J. Coal Geol.* **2012**, *95*, 34−46.
(132) Ross, D. J. K.; Marc Bustin, R. Impact of Mass Balance Calculations on Adsorption Capacities in Microporous Shale Gas Reservoirs. *Fuel* **2007**, *86* (17−18), 2696−2706.
(133) Chalmers, G. R. L.; Bustin, R. M. The Organic Matter Distribution and Methane Capacity of the Lower Cretaceous Strata of Northeastern British Columbia, Canada. *Int. J. Coal Geol.* **2007**, *70*, 223−239.
(134) Varma, A. K.; Hazra, B.; Samad, S. K.; Panda, S.; Mendhe, V. A. Methane Sorption Dynamics and Hydrocarbon Generation of Shale Samples from West Bokaro and Raniganj Basins, India. *J. Nat. Gas Sci. Eng.* **2014**, *21*, 1138−1147.
(135) Charoensuppanimit, P.; Mohammad, S. A.; Gasem, K. A. M. Measurements and Modeling of Gas Adsorption on Shales. *Energy Fuels* **2016**, *30* (3), 2309−2319.
(136) Gasparik, M.; Ghanizadeh, A.; Bertier, P.; Gensterblum, Y.; Bouw, S.; Krooss, B. M. High-Pressure Methane Sorption Isotherms of Black Shales from the Netherlands. *Energy Fuels* **2012**, *26* (8), 4995−5004.
(137) Hazra, B.; Varma, A. K.; Bandopadhyay, A. K.; Mendhe, V. A.; Singh, B. D.; Saxena, V. K.; Samad, S. K.; Mishra, D. K. Petrographic Insights of Organic Matter Conversion of Raniganj Basin Shales, India. *Int. J. Coal Geol.* **2015**, *150−151*, 193−209.
(138) Kang, S. M.; Fathi, E.; Ambrose, R. J.; Akkutlu, I. Y.; Sigal, R. F. Carbon Dioxide Storage Capacity of Organic-Rich Shales. *SPE J.* **2011**, *16* (4), 842−855.
(139) Duan, S.; Gu, M.; Du, X.; Xian, X. Adsorption Equilibrium of CO_2 and CH_4 and their mixture on Sichuan Basin Shale. *Energy Fuels* **2016**, *30* (3), 2248−2256.
(140) Klewiah, I.; Berawala, D. S.; Alexander Walker, H. C.; Andersen, P.; Nadeau, P. H. Review of Experimental Sorption Studies of CO_2 and CH_4 in Shales. *J. Nat. Gas Sci. Eng.* **2020**, *73*, 103045.
(141) Guo, S. Experimental Study on Isothermal Adsorption of Methane Gas on Three Shale Samples from Upper Paleozoic Strata of the Ordos Basin. *J. Pet. Sci. Eng.* **2013**, *110*, 132−138.
(142) Curtis, M. E.; Sondergeld, C. H.; Ambrose, R. J.; Rai, C. S. Microstructural Investigation of Gas Shales in Two and Three Dimensions Using Nanometer-Scale Resolution Imaging. *Am. Assoc. Pet. Geol. Bull.* **2012**, *96* (4), 665−677.
(143) Curtis, M. E.; Cardott, B. J.; Sondergeld, C. H.; Rai, C. S. Development of Organic Porosity in the Woodford Shale with Increasing Thermal Maturity. *Int. J. Coal Geol.* **2012**, *103*, 26−31.
(144) Bernard, S.; Horsfield, B.; Schulz, H. M.; Wirth, R.; Schreiber, A.; Sherwood, N. Geochemical Evolution of Organic-Rich Shales with Increasing Maturity: A STXM and TEM Study of the Posidonia Shale (Lower Toarcian, Northern Germany). *Mar. Pet. Geol.* **2012**, *31* (1), 70−89.
(145) Mastalerz, M.; He, L.; Melnichenko, Y. B.; Rupp, J. A. Porosity of Coal and Shale: Insights from Gas Adsorption and SANS/USANS Techniques. *Energy Fuels* **2012**, *26* (8), 5109−5120.
(146) Mastalerz, M.; Hampton, L. B.; Drobniak, A.; Loope, H. Significance of Analytical Particle Size in Low-Pressure N2 and CO_2 Adsorption of Coal and Shale. *Int. J. Coal Geol.* **2017**, *178*, 122−131.
(147) Milliken, K. L.; Rudnicki, M.; Awwiller, D. N.; Zhang, T. Organic Matter-Hosted Pore System, Marcellus Formation (Devonian), Pennsylvania. *Am. Assoc. Pet. Geol. Bull.* **2013**, *97* (2), 177−200.
(148) Bernard, S.; Horsfield, B. Thermal Maturation of Gas Shale Systems. *Annu. Rev. Earth Planet. Sci.* **2014**, *42*, 635−651.
(149) Pommer, M.; Milliken, K. Pore Types and Pore-Size Distributions across Thermal Maturity, Eagle Ford Formation, Southern Texas. *Am. Assoc. Pet. Geol. Bull.* **2015**, *99* (9), 1713−1744.
(150) Dong, T.; Harris, N. B.; Ayranci, K.; Twemlow, C. E.; Nassichuk, B. R. Porosity Characteristics of the Devonian Horn River Shale, Canada: Insights from Lithofacies Classification and Shale Composition. *Int. J. Coal Geol.* **2015**, *141−142*, 74−90.

https://doi.org/10.1021/acs.energyfuels.2c01894
Energy Fuels 2022, 36, 9882−9903

(151) Holmes, R.; Rupp, E. C.; Vishal, V.; Wilcox, J. Selection of Shale Preparation Protocol and Outgas Procedures for Applications in Low-Pressure Analysis. *Energy Fuels* **2017**, *31* (9), 9043−9051.
(152) Hazra, B.; Wood, D. A.; Vishal, V.; Singh, A. K. Pore characteristics of distinct thermally mature shales: influence of particle size on low-pressure CO_2 and N_2 adsorption. *Energy Fuels* **2018**, *32*, 8175−8186.
(153) Hazra, B.; Chandra, D.; Singh, A. K.; Varma, A. K.; Mani, D.; Singh, P. K.; Boral, P.; Buragohain, J. Comparative Pore Structural Attributes and Fractal Dimensions of Lower Permian Organic-Matter-Bearing Sediments of Two Indian Basins: Inferences from Nitrogen Gas Adsorption. *Energy Sources, Part A Recover. Util. Environ. Eff.* **2019**, *41* (24), 2975−2988.
(154) Chandra, D.; Vishal, V.; Bahadur, J.; Sen, D. A Novel Approach to Identify Accessible and Inaccessible Pores in Gas Shales Using Combined Low-Pressure Sorption and SAXS/SANS Analysis. *Int. J. Coal Geol.* **2020**, *228*, No. 103556.
(155) Chandra, D.; Vishal, V.; Bahadur, J.; Agrawal, A. K.; Das, A.; Hazra, B.; Sen, D. Nano-scale physicochemical attributes and their impact on pore heterogeneity in shale. *Fuel* **2022**, *314*, 123070.
(156) Chandra, D.; Vishal, V. A Comparison of Nano-Scale Pore Attributes of Barakar Formation Gas Shales from Raniganj and Wardha Basin, India Using Low Pressure Sorption and FEG-SEM Analysis. *J. Nat. Gas Sci. Eng.* **2020**, *81*, No. 103453.
(157) Singh, D. P.; Chandra, D.; Vishal, V.; Hazra, B.; Sarkar, P. Impact of degassing time and temperature on the estimation of pore attributes in shale. *Energy Fuels* **2021**, *35* (19), 15628−15641.
(158) Gu, X.; Mildner, D. F.; Cole, D. R.; Rother, G.; Slingerland, R.; Brantley, S. L. Quantification of organic porosity and water accessibility in Marcellus shale using neutron scattering. *Energy Fuels* **2016**, *30* (6), 4438−4449.
(159) Leu, L.; Georgiadis, A.; Blunt, M. J.; Busch, A.; Bertier, P.; Schweinar, K.; Liebi, M.; Menzel, A.; Ott, H. Multiscale description of shale pore systems by scanning SAXS and WAXS microscopy. *Energy Fuels* **2016**, *30* (12), 10282−10297.
(160) Hazra, B.; Wood, D. A.; Kumar, S.; Saha, S.; Dutta, S.; Kumari, P.; Singh, A. K. Fractal disposition, porosity characterization and relationships to thermal maturity for the Lower Permian Raniganj basin shales, India. *J. Nat. Gas Sci. Eng.* **2018**, *59*, 452−465.
(161) Chandra, D.; Vishal, V. A critical review on pore to continuum scale imaging techniques for enhanced shale gas recovery. *Earth Sci. Rev.* . **2021**, *217*, 103638.
(162) Hosseini, M.; Arif, M.; Keshavarz, A.; Iglauer, S. Neutron scattering: A subsurface application review. *Earth Sci. Rev.* . **2021**, *221*, 103755.
(163) Liu, B.; Schieber, J.; Mastalerz, M. Combined SEM and reflected light petrography of organic matter in the New Albany Shale (Devonian-Mississippian) in the Illinois Basin: A perspective on organic pore development with thermal maturation. *Int. J. Coal Geol.* **2017**, *184*, 57−72.
(164) Saif, T.; Lin, Q.; Butcher, A. R.; Bijeljic, B.; Blunt, M. J. Multi-scale multi-dimensional microstructure imaging of oil shale pyrolysis using X-ray micro-tomography, automated ultra-high resolution SEM, MAPS Mineralogy and FIB-SEM. *Appl. Energy* **2017**, *202*, 628−647.
(165) Hazra, B.; Wood, D. A.; Mani, D.; Singh, P. K.; Singh, A. K. Organic and inorganic porosity, and controls of hydrocarbon storage in shales. In *Evaluation of Shale Source Rocks and Reservoirs*; Springer: Cham, Switzerland, 2019; pp 107−138.
(166) Petrovic, B.; Gorbounov, M.; Soltani, S. M. Impact of Surface Functional Groups and Their Introduction Methods on the Mechanisms of CO_2 Adsorption on Porous Carbonaceous Adsorbents. *Carbon Capture Sci. Technol.* **2022**, 1−63.
(167) Loucks, R. G.; Reed, R. M.; Ruppel, S. C.; Hammes, U. Spectrum of Pore Types and Networks in Mudrocks and a Descriptive Classification for Matrix-Related Mudrock Pores. *Am. Assoc. Pet. Geol. Bull.* **2012**, *96* (6), 1071−1098.
(168) Zhang, T.; Ellis, G. S.; Ruppel, S. C.; Milliken, K.; Yang, R. Effect of Organic-Matter Type and Thermal Maturity on Methane Adsorption in Shale-Gas Systems. *Org. Geochem.* **2012**, *47*, 120−131.
(169) Merey, S.; Sinayuc, C. Analysis of Carbon Dioxide Sequestration in Shale Gas Reservoirs by Using Experimental Adsorption Data and Adsorption Models. *J. Nat. Gas Sci. Eng.* **2016**, *36*, 1087−1105.
(170) Delle Piane, C.; Sarout, J. Effects of Water and Supercritical CO_2 on the Mechanical and Elastic Properties of Berea Sandstone. *Int. J. Greenh. Gas Control* **2016**, *55*, 209−220.
(171) Lu, Y.; Chen, X.; Tang, J.; Li, H.; Zhou, L.; Han, S.; Ge, Z.; Xia, B.; Shen, H.; Zhang, J. Relationship between Pore Structure and Mechanical Properties of Shale on Supercritical Carbon Dioxide Saturation. *Energy* **2019**, *172*, 270−285.
(172) Su, E.; Liang, Y.; Chang, X.; Zou, Q.; Xu, M.; Sasmito, A. P. Effects of Cyclic Saturation of Supercritical CO_2 on the Pore Structures and Mechanical Properties of Bituminous Coal: An Experimental Study. *J. CO_2 Util.* **2020**, *40* (May), No. 101208.
(173) Bai, B.; Ni, H. J.; Shi, X.; Guo, X.; Ding, L. The Experimental Investigation of Effect of Supercritical CO_2 Immersion on Mechanical Properties and Pore Structure of Shale. *Energy* **2021**, *228*, 120663.
(174) Alqahtani, A. A.; Mokhtari, M.; Tutuncu, A. N.; Sonnenberg, S. Effect of Mineralogy and Petrophysical Characteristics on Acoustic and Mechanical Properties of Organic Rich Shale. *Unconv. Resour. Technol. Conf. 2013, URTC* **2013**, 399−411.
(175) Yin, H.; Zhou, J.; Xian, X.; Jiang, Y.; Lu, Z.; Tan, J.; Liu, G. Experimental Study of the Effects of Sub- and Super-Critical CO_2 Saturation on the Mechanical Characteristics of Organic-Rich Shales. *Energy* **2017**, *132*, 84−95.
(176) Zou, Y.; Li, N.; Ma, X.; Zhang, S.; Li, S. Experimental Study on the Growth Behavior of Supercritical CO_2-Induced Fractures in a Layered Tight Sandstone Formation. *J. Nat. Gas Sci. Eng.* **2018**, *49*, 145−156.
(177) Lyu, Q.; Long, X.; Pg, R.; Tan, J.; Zhou, J.; Wang, Z.; Luo, W. A Laboratory Study of Geomechanical Characteristics of Black Shales after Sub-Critical/Super-Critical CO_2 + Brine Saturation. *Geomech. Geophys. Geo-Energy Geo-Resources* **2018**, *4* (2), 141−156.
(178) Choi, C. S.; Kim, J.; Song, J. J. Analysis of Shale Property Changes after Geochemical Interaction under CO_2 Sequestration Conditions. *Energy* **2021**, *214*, No. 118933.
(179) Lyu, Q.; Long, X.; Ranjith, P. G.; Tan, J.; Kang, Y.; Wang, Z. Experimental Investigation on the Mechanical Properties of a Low-Clay Shale with Different Adsorption Times in Sub-/Super-Critical CO_2. *Energy* **2018**, *147*, 1288−1298.
(180) Lyu, Q.; Long, X.; Ranjith, P. G.; Kang, Y. Unconventional Gas: Experimental Study of the Influence of Subcritical Carbon Dioxide on the Mechanical Properties of Black Shale. *Energies* **2016**, *9* (7), 516.
(181) Pimienta, L.; Esteban, L.; Sarout, J.; Liu, K.; Dautriat, J.; Delle Piane, C.; Clennell, M. B. Supercritical CO_2 Injection and Residence Time in Fluid-Saturated Rocks: Evidence for Calcite Dissolution and Effects on Rock Integrity. *Int. J. Greenh. Gas Control* **2017**, *67*, 31−48.
(182) Guha Roy, D.; Singh, T. N.; Kodikara, J.; Das, R. Effect of Water Saturation on the Fracture and Mechanical Properties of Sedimentary Rocks. *Rock Mech. Rock Eng.* **2017**, *50* (10), 2585−2600.
(183) Ao, X.; Lu, Y.; Tang, J.; Chen, Y.; Li, H. Investigation on the Physics Structure and Chemical Properties of the Shale Treated by Supercritical CO_2. *J. CO_2 Util.* **2017**, *20*, 274−281.
(184) Feng, G.; Kang, Y.; Sun, Z.-d.; Wang, X.-c.; Hu, Y.-q. Effects of Supercritical CO_2 Adsorption on the Mechanical Characteristics and Failure Mechanisms of Shale. *Energy* **2019**, *173*, 870−882.
(185) Lu, Y.; Xu, Z.; Li, H.; Tang, J.; Chen, X. The Influences of Super-Critical CO_2 Saturation on Tensile Characteristics and Failure Modes of Shales. *Energy* **2021**, *221*, No. 119824.
(186) Shi, X.; Jiang, S.; Wang, Z.; Bai, B.; Xiao, D.; Tang, M. Application of Nanoindentation Technology for Characterizing the Mechanical Properties of Shale before and after Supercritical CO_2 Fluid Treatment. *J. CO_2 Util.* **2020**, *37*, 158−172.
(187) Meng, S.; Jin, X.; Tao, J.; Wang, X.; Zhang, C. Evolution Characteristics of Mechanical Properties under Supercritical Carbon Dioxide Treatment in Shale Reservoirs. *ACS Omega* **2021**, *6* (4), 2813−2823.

https://doi.org/10.1021/acs.energyfuels.2c01894
Energy Fuels 2022, 36, 9882−9903

(188) Qin, C.; Jiang, Y.; Kang, Z.; Song, X.; Liu, H. Experimental Study on Tensile Strength and Acoustic Emission Characteristics of Shale Exposure to Supercritical CO_2. *Energy Sources, Part A Recover. Util. Environ. Eff.* **2021**, *43* (8), 977−992.
(189) Song, W.; Ni, H.; Tang, P.; Zhang, S.; Gao, J.; Zhang, J.; Shen, B. Simulation of Supercritical Carbon Dioxide Fracturing in Shale Gas Reservoir. *J. Therm. Sci.* **2021**, *30* (4), 1444−1451.
(190) Zhou, J.; Tian, S.; Zhou, L.; Xian, X.; Yang, K.; Jiang, Y.; Zhang, C.; Guo, Y. Experimental Investigation on the Influence of Sub- and Super-Critical CO_2 Saturation Time on the Permeability of Fractured Shale. *Energy* **2020**, *191*, No. 116574.
(191) Lyu, Q.; Wang, K.; Wanniarachchi, W. A. M.; Hu, C.; Shi, J. Hydro-Mechanical Properties of a Low-Clay Shale with Supercritical CO_2 Imbibition. *Geomech. Geophys. Geo-Energy Geo-Resources* **2020**, *6* (4), 69.
(192) King, G. E. Thirty years of gas shale fracturing: what have we learned? Presented at the *SPE Annual Technical Conference and Exhibition*, Florence, Italy, Sept. 19−22, 2010. Paper No. SPE 133456.
(193) Veytskin, Y. B.; Tammina, V. K.; Bobko, C. P.; Hartley, P. G.; Clennell, M. B.; Dewhurst, D. N.; Dagastine, R. R. Micromechanical Characterization of Shales through Nanoindentation and Energy Dispersive X-Ray Spectrometry. *Geomech. Energy Environ.* **2017**, *9*, 21−35.
(194) Ougier-Simonin, A.; Renard, F.; Boehm, C.; Vidal-Gilbert, S. Microfracturing and microporosity in shales. *Earth Sci. Rev.* . **2016**, *162*, 198−226.
(195) Fatah, A.; Bennour, Z.; Ben Mahmud, H.; Gholami, R.; Hossain, M. A review on the influence of CO_2/shale interaction on shale properties: implications of CCS in shales. *Energies* **2020**, *13* (12), 3200.
(196) Arif, M.; Mahmoud, M.; Zhang, Y.; Iglauer, S. X-ray tomography imaging of shale microstructures: A review in the context of multiscale correlative imaging. *Int. J. Coal Geol.* **2021**, *233*, 103641.
(197) Jarvie, D. M. Shale resource systems for oil and gas: Part 2—Shale-oil resource systems. In *Shale Reservoirs—Giant Resources for the 21st Century: AAPG Memoir*; Breyer, J. A., Ed.; AAPG, 2012; Vol. *97*, pp 89−119.
(198) Sondergeld, C. H.; Ambrose, R. J.; Rai, C. S.; Moncrieff, J. Microstructural studies of gas shales. Presented at the *SPE Unconventional Gas Conference*, Feb. 23−25, 2010, Pittsburgh, PA, Paper No. SPE-131771.
(199) Kuila, U.; Prasad, M. Specific surface area and pore-size distribution in clays and shales. *Geophys. Prospect.* **2013**, *61* (2), 341−362.
(200) Sakhaee-Pour, A.; Bryant, S. L. Gas permeability of shale. *SPE Reservoir Eval. Eng.* **2012**, *15* (04), 401−409.
(201) Jiang, Y.; Luo, Y.; Lu, Y.; Qin, C.; Liu, H. Effects of Supercritical CO_2 Treatment Time, Pressure, and Temperature on Microstructure of Shale. *Energy* **2016**, *97*, 173−181.
(202) Pan, Y.; Hui, D.; Luo, P.; Zhang, Y.; Zhang, L.; Sun, L. Influences of Subcritical and Supercritical CO_2 Treatment on the Pore Structure Characteristics of Marine and Terrestrial Shales. *J. CO_2 Util.* **2018**, *28*, 152−167.
(203) Dai, X.; Wang, M.; Wei, C.; Zhang, J.; Wang, X.; Zou, M. Factors Affecting Shale Microscopic Pore Structure Variation during Interaction with Supercritical CO_2. *J. CO_2 Util.* **2020**, *38*, 194−211.
(204) Ozotta, O.; Liu, K.; Gentzis, T.; Carvajal-Ortiz, H.; Liu, B.; Rafieepour, S.; Ostadhassan, M. Pore Structure Alteration of Organic-Rich Shale with SC-CO_2 Exposure: The Bakken Formation. *Energy Fuels* **2021**, *35* (6), 5074−5089.
(205) Sanguinito, S.; Goodman, A.; Tkach, M.; Kutchko, B.; Culp, J.; Natesakhawat, S.; Fazio, J.; Fukai, I.; Crandall, D. Quantifying Dry Supercritical CO_2-Induced Changes of the Utica Shale. *Fuel* **2018**, *226*, 54−64.
(206) Cheng, Y.; Zeng, M.; Lu, Z.; Du, X.; Yin, H.; Yang, L. Effects of Supercritical CO_2 Treatment Temperatures on Mineral Composition, Pore Structure and Functional Groups of Shale: Implications for CO_2 Sequestration. *Sustain.* **2020**, *12* (9), 3927.
(207) Qin, C.; Jiang, Y.; Zhou, J.; Zuo, S.; Chen, S.; Liu, Z.; Yin, H.; Li, Y. Influence of Supercritical CO_2 Exposure on Water Wettability of Shale: Implications for CO_2 Sequestration and Shale Gas Recovery. *Energy* **2022**, *242*, 122551.
(208) Luo, X.; Ren, X.; Wang, S. Supercritical CO_2-Water-Shale Interactions and Their Effects on Element Mobilization and Shale Pore Structure during Stimulation. *Int. J. Coal Geol.* **2019**, *202*, 109−127.
(209) Wang, S.; Liu, K.; Han, J.; Ling, K.; Wang, H.; Jia, B. Investigation of Properties Alternation during Super-Critical CO_2 Injection in Shale. *Appl. Sci.* **2019**, *9* (8), 1686.
(210) Hui, D.; Pan, Y.; Luo, P.; Zhang, Y.; Sun, L.; Lin, C. Effect of Supercritical CO_2 Exposure on the High-Pressure CO_2 Adsorption Performance of Shales. *Fuel* **2019**, *247* (March), 57−66.
(211) Rezaee, R.; Saeedi, A.; Iglauer, S.; Evans, B. Shale Alteration after Exposure to Supercritical CO_2. *Int. J. Greenh. Gas Control* **2017**, *62*, 91−99.
(212) Huang, X.; Zhao, Y. P.; Wang, X.; Pan, L. Adsorption-Induced Pore Blocking and Its Mechanisms in Nanoporous Shale Due to Interactions with Supercritical CO_2. *J. Pet. Sci. Eng.* **2019**, *178*, 74−81.
(213) Wang, S.; Javadpour, F.; Feng, Q. Fast Mass Transport of Oil and Supercritical Carbon Dioxide through Organic Nanopores in Shale. *Fuel* **2016**, *181*, 741−758.
(214) Sun, X.; Dai, C.; Sun, Y.; Du, M.; Wang, T.; Zou, C.; He, J. Wettability alteration study of supercritical CO_2 fracturing fluid on low permeability oil reservoir. *Energy Fuels* **2017**, *31* (12), 13364−13373.
(215) Arif, M.; Al-Yaseri, A. Z.; Barifcani, A.; Lebedev, M.; Iglauer, S. Impact of pressure and temperature on CO_2−brine−mica contact angles and CO_2−brine interfacial tension: Implications for carbon geo-sequestration. *J. Colloid Interface Sci.* **2016**, *462*, 208−215.
(216) Arif, M.; Barifcani, A.; Lebedev, M.; Iglauer, S. Impact of solid surface energy on wettability of CO_2-brine-Mineral systems as a function of pressure, temperature and salinity. *Energy Procedia* **2017**, *114*, 4832−4842.
(217) Arif, M.; Abu-Khamsin, S. A.; Iglauer, S. Wettability of rock/CO_2/brine and rock/oil/CO_2-enriched-brine systems: Critical parametric analysis and future outlook. *Adv. Colloid Interface Sci.* **2019**, *268*, 91−113.
(218) Arif, M.; Zhang, Y.; Iglauer, S. Shale wettability: Data sets, challenges, and outlook. *Energy Fuels* **2021**, *35* (4), 2965−2980.
(219) Zhu, Z.; Li, M.; Lin, M.; Peng, B.; Sun, L.; Chen, L. Investigation on variations in wettability of reservoir rock induced by CO_2−brine−rock interactions. In *SPE EUROPEC/EAGE Annual Conference and Exhibition*; Vienna, Austria, 2011; Society of Petroleum Engineers; Vol. *5*, pp 4027−4038.
(220) Khan, J. A.; Padmanabhan, E.; Haq, I. U.; Yekeen, N.; Mumtaz, M.; Prajapati, S. Experimental Assessment of Fracture Initiation and Wettability in Low and High Brittle Shales by CO_2 Foam Fracturing Fluids. *Energy Fuels* **2022**, *36*, 8288.
(221) Kaveh, N. S.; Barnhoorn, A.; Wolf, K. H. Wettability evaluation of silty shale caprocks for CO_2 storage. *Int. J. Greenh. Gas Control.* **2016**, *49*, 425−435.
(222) Fatah, A.; Mahmud, H. B.; Bennour, Z.; Hossain, M.; Gholami, R. Effect of supercritical CO_2 treatment on physical properties and functional groups of shales. *Fuel* **2021**, *303*, 121310.
(223) Fatah, A.; Bennour, Z.; Mahmud, H. B.; Gholami, R.; Hossain, M. Surface wettability alteration of shales exposed to CO_2: Implication for long-term integrity of geological storage sites. *Int. J. Greenh. Gas Control.* **2021**, *110*, 103426.
(224) Guiltinan, E. J.; Cardenas, M. B.; Bennett, P. C.; Zhang, T.; Espinoza, D. N. The effect of organic matter and thermal maturity on the wettability of supercritical CO_2 on organic shales. *Int. J. Greenh. Gas Control.* **2017**, *65*, 15−22.
(225) Fatah, A.; Ben Mahmud, H.; Bennour, Z.; Gholami, R.; Hossain, M. The Impact of Supercritical CO_2 on the Pore Structure and Storage Capacity of Shales. *J. Nat. Gas Sci. Eng.* **2022**, *98*, No. 104394.
(226) Wang, T.; Wang, Q.; Zhang, P.; Cheng, S.; Anyimah, P. O.; Tan, Y.; Tian, S. Application of atom force microscope and nanoindentation to characterize nanoscale mechanical properties of shale before and after supercritical CO_2 immersion. *J. Pet. Sci. Eng.* **2022**, *212*, 110348.
(227) Singh, D. P.; Singh, V.; Singh, P. K.; Hazra, B. Source rock properties and pore structural features of distinct thermally mature

https://doi.org/10.1021/acs.energyfuels.2c01894
Energy Fuels 2022, 36, 9882−9903

Permian shales from South Rewa and Jharia basins, India. *Arab. J. Geosci.* **2021**, *14* (10), 916.
(228) Singh, D. P.; Wood, D. A.; Hazra, B.; Singh, P. K. Pore Properties in Organic-Rich Shales Derived Using Multiple Fractal Determination Models Applied to Two Indian Permian Basins. *Energy Fuels* **2021**, *35* (18), 14618−14633.
(229) Zhou, J.; Liu, G.; Jiang, Y.; Xian, X.; Liu, Q.; Zhang, D.; Tan, J. Supercritical carbon dioxide fracturing in shale and the coupled effects on the permeability of fractured shale: an experimental study. *J. Nat. Gas Sci. Eng.* **2016**, *36*, 369−377.
(230) Memon, S.; Feng, R.; Ali, M.; Bhatti, M. A.; Giwelli, A.; Keshavarz, A.; Xie, Q.; Sarmadivaleh, M. Supercritical CO_2-Shale interaction induced natural fracture closure: Implications for $scCO_2$ hydraulic fracturing in shales. *Fuel* **2022**, *313*, 122682.
(231) Rogers, R. *Coalbed Methane: Principles and Practices*; The Prentice Hall Professional, Technical, and Reference Division, 1994.
(232) Larson, R. G.; Scriven, L. E.; Davis, H. T. Percolation theory of two phase flow in porous media. *Chem. Eng. Sci.* **1981**, *36* (1), 57−73.
(233) Lucena, L. S.; Freitas, J. E.; Corso, G.; Soares, R. F. Anisotropy and percolation threshold in a multifractal support. *Braz. J. Phys.* **2003**, *33* (3), 637−640.
(234) Masihi, M.; King, P. R.; Nurafza, P. Effect of anisotropy on finite-size scaling in percolation theory. *Phys. Rev. E* **2006**, *74* (4), No. 042102.
(235) Sadeghnejad, S.; Masihi, M.; King, P. R.; Shojaei, A.; Pishvaei, M. Effect of anisotropy on the scaling of connectivity and conductivity in continuum percolation theory. *Phys. Rev. E* **2010**, *81* (6), No. 061119.
(236) Lu, Y.; Tian, R.; Tang, J.; Jia, Y.; Lu, Z.; Sun, X. Investigating the Mineralogical and Chemical Effects of CO_2 Injection on Shale Wettability at Different Reservoir Temperatures and Pressures. *Energy Fuels* **2021**, *35* (18), 14838−14851.
(237) Pan, B.; Li, Y.; Wang, H.; Jones, F.; Iglauer, S. CO_2 and CH_4 wettabilities of organic-rich shale. *Energy Fuels* **2018**, *32* (2), 1914−1922.
(238) Pan, B.; Ni, T.; Zhu, W.; Yang, Y.; Ju, Y.; Zhang, L.; Chen, S.; Gu, J.; Li, Y.; Iglauer, S. Mini Review on Wettability in the Methane−Liquid−Rock System at Reservoir Conditions: Implications for Gas Recovery and Geo-Storage. *Energy Fuels* **2022**, *36* (8), 4268−4275.

https://doi.org/10.1021/acs.energyfuels.2c01894
Energy Fuels 2022, 36, 9882−9903